Time-Predictable Fault Modeling of Bangladesh

June 2009

UKaid
from the British people

European Union

NORWEGIAN EMBASSY

SWEDEN

Australian AID

UNDP
Empowered lives.
Resilient nations.

Time-Predictable Fault Modeling of Bangladesh

Time-Predictable Fault Modeling of Bangladesh

June 2009

TIME-PREDICTABLE FAULT MODELING
FOR
SEISMIC HAZARD
AND VULNERABILITY ASSESSMENT
OF
DHAKA, CHITTAGONG AND SYLHET
CITY CORPORATION AREA

JUNE 2009

Asian Disaster Preparedness Center

OYO International Corporation

Executive Summary

The time-predictable fault models for seismic strong ground motion estimation in Dhaka, Chittagong and Sylhet were established based on the seismic data, existing literatures, and trench investigation in this project.

The Indian Plate is moving toward north-east with slip rate of 6 cm/year and subducting under Eurasian Plate along Himalaya Arc and subduction zone continuing from off Sumatra. The shapes of east ward subducting plate boundaries are clearly found on the depth section of epicenter. Large earthquakes occurred historically along the subduction fault, namely the 1762 earthquake and the 2004 Mw 9.2 off Sumatra earthquake. Shillong Plateau is located in the north of Bangladesh. The E-W trending Dauki Fault, which is a reverse one dipping to the north, is distributed on the southern fringe of Shillong Plateau.

The seismicity study is based on the earthquake catalogue of BUET from 1664 to recent period. The source zone was divided into three zones of north and east plate subduction zones with high seismicity and relatively low active shallow crustal zone including main Bangladesh. The b-value for the shallow crustal zone is 0.84, eastern subduction zone is 0.96 and for northern subduction zone is 0.92.

The historical earthquakes in Bangladesh and its surroundings areas were studied based on several historical catalogues and literatures. The historical earthquakes that are analyzed for the study are, the *1548 Earthquake:* may relate with subducting eastern edge of Indian Plate; the *1664 Earthquake:* general source area may beneath Shillong Plateau; the *1762 Earthquake:* occurred on the northern extension of the 2004 Sumatra earthquake; the *1869 Cachar earthquake:* source area is around Sylhet; the *1885 Bengal Earthquake:* source area is north-west of Dhaka; the *1897 Great Assam Earthquake:* source area is around Shillong Plateau and the *1918 Srimangal Earthquake:* source area is around Sylhet. There are also other recorded earthquakes with magnitude between 7.0 and 7.4. However, the earthquakes of 1642, 1812, 1842, 1923 and 1930 could not be identified the relation with the faults, but the 1918 earthquake could be due to the plate boundary fault 2 (PBF-2), the 1869 earthquake could be due to PBF-3, and earthquakes of 1943, 1954, 1988 could be due to Dauki Fault.

After the interpretation of CORONA satellite images of entire Bangladesh, several sites were selected as the target of active fault surveys. The sites where field survey were carried out including *(1) Maheskhali*: A straight N-S trending low fault scarp was identified; *(2) Chittagong:* The topographic boundary between hill and plain was not estimated as active fault by CORONA photo interpretation and it was inferred to be the eroded scarp by field survey. The drilling data indicates Chittagong is located on the hanging wall of the plate boundary fault through the off Chittagong; *(3) Feni:* The narrow longitudinal N-S trending hill is located in the north of Feni. The uplifted terraces are recognized on the western edge of the hill. The plate boundary fault is inferred on the topographic boundary between the terrace and alluvial plain, *(4) Comilla and Shazi Bazar:* The hill is located in the west of Comilla Town and the terrace is recognized on the western edge of the hill. However, the terrace may be fluvial, not uplifted one. The plate boundary fault may be concealed in Comilla, *(5) Saestagonj:* The N-S trending low warping scarp is confirmed in the alluvial plain, about 500m west from the topographic boundary between the hill and alluvial plain, on the CORONA photo as well as in the field. However, the plate boundary fault may be concealed, since the warping scarp is very gentle and wide with the height of 1-2 m, *(6) Sylhet:* The low scarp was identified at the northeast of Sylhet, which is located on the southern edge of the hills extended from Shillong Plateau, on the CORONA photo. However, the geomorphic features and exposure indicative of an active fault (Dauki Fault) was not confirmed in the field. The warping scarp was inferred on the side of

alluvial fan located in the north of Chhatak. The Dauki Fault was inferred to cross the alluvial fan. Though, the warping scarp was not confirmed in the field, the scarp may have been modified by cultivation, *(7) Haluaghat:* The narrow terraces were identified on the southern edge of the hills in the north of Haluaghat. The Dauki Fault is inferred on the topographic boundary between the terrace and alluvial plain, since the terrace is estimated to be uplifted alluvial plain. The back-tilting terrace, which was created by the activity of the Dauki Fault, was confirmed at Gabrakhari Village, *(8) Northwest of Sherpur:* The uplifted terraces were identified in the northwest of Sherpur as the north of Haluaghat. However, the field survey could not be carried out, since the region is located near the border, *(9) Madhupur:* The straight NNW-SSE trending low scarp is identified on the western edge of Madhupur block on the CORONA photo. However, it is inferred to be the eroded one. Madhupur Fault may be concealed, *(10) Saidpur:* Nakata and Kumahar (2002) suggested a right-lateral fault around Saidpur. The low scarp is identified in the southwest of Saidpur Town by the CORONA photo interpretation as well as the field survey.

Trench investigation was carried out in four sites to clarify the detailed characteristics of the faults. This kind of trenching survey is the first attempt in Bangladesh, and it provided extraordinary results on the characteristics of active faults in Bangladesh. *(1) Gabrakhari Trench across the Dauki Fault:* Four trenches were excavated at Gabrakhari Village. The Dauki Fault was confirmed at Gabrakhari 1 site. The gentle warping structure was recognized at Gabrakhari 2 site, and the paleo-liquefaction was found out at Awlatory Village. The trench at Gabrakhari 1 site was excavated on the southern edge of the back-tilting terrace. Two events were identified in the trench. The latest event corresponds with the 1897 Great Assam earthquake, since the historical earthquake which occurred along the Dauki fault after AD 1700 is only the 1897 earthquake. It is estimated that the penultimate event occurred during AD1500 to 1640. The penultimate event may correspond with the 1548 earthquake. The paleo-liquefaction confirmed at Awlatory Village is inferred to be created during the 1897 earthquake, *(2) Feni Trench across the Plate Boundary Fault:* Two trenches were excavated. The fault was concealed at both sites and only warping structure was observed. Two events were inferred. The time of last event is unknown and the time of penultimate event is considered to have occurred during BC 90 and AD 70. Shishikura et al. (2008, 2009) studied the uplifted marine terraces on the Islands of off Myanmar. According to their studies, the four events were identified, namely AD1762, AD680-980, BC150–AD50 and BC1395-740. This suggests that the recurrence period of the subduction fault is about 900 years and the third event by Shishikura et al. (2008, 2009) is coincident with the penultimate event at above Feni site, *(3) Saestagonj Trench across the Plate Boundary Fault:* The trench investigation at two sites was carried out. However, an active fault could not be confirmed. It is thought that an active fault is concealed around Saestagonj. Instead the crater, which is a kind of liquefaction, was found out at Hobigonj Village. According to the radiocarbon ages collected in the trench, the formation of the crater is dated back to about Cal BC 1000. The fourth event along the subduction fault by Shishikura et al. (2008, 2009) is inferred to have occurred during Cal BC 1395 to 740. The crater may have been formed by this earthquake, *(4) Saidpur Trench:* The trench was planned in Saidpur. However, only small trench (pilot trench) was excavated, since the rice before harvest was planted at the trench site. Any deformation of the stratigraphy indicative of active fault could not be confirmed in the pilot trench. Larger trench should be tried on December to January in future when rice is not planted.

Conclusion

Based on above data and information, time-predictable fault model, as the current most, was established as follows. This was made based on the limited currently available information and should be revised in the future.

Plate Boundary Fault 1 (PBF1)

According to Shishikura et al. (2008, 2009), the latest event along PBF occurred during the 1762 earthquake and the recurrence period is 900 years. The 50 years probability of future earthquake occurrence is 1.1 %, which is small, because the elapsed time since the latest event is 246 years and the recurrence period is 900 years.

Plate Boundary Fault 2 and 3 (PBF2 and PBF3)

The latest event and the recurrence period along the PBF2 and PBF3 are unknown. If the recurrence period is 900 years by analogy with PBF1 and the latest event is before 16th century, 50 years probability is over 6.7 %.

Dauki Fault (DF)

The latest event corresponds with the 1897 Great Assam Earthquake. The time of the penultimate event is inferred to correspond with the 1548 earthquake. Since the recurrence period is 349 years and the elapsed time is 111 years, the 50 years probability is 7.0 %.

Madhupur Blind Fault (MF)

The 1885 earthquake (Ms7.0) is regarded as the latest event for characteristic earthquake on the Madhupur Fault based on the existing documents. The recurrence period is unknown. If the recurrence period is 350 years by analogy with the Dauki Fault, the 50 years probability is 8.7 %.

Table of Contents

List of Figure

List of Table

1. Introduction

Bangladesh has suffered severe damages from large earthquakes historically, viz., the 1548 earthquake, the 1664 earthquake, the 1762 earthquake, the 1869 Cachen earthquake (Ms 7.5), the 1885 Bengal earthquake (Ms 7.0), the 1897 Great Assam earthquake (Ms 8.1), and the 1918 Srimangal earthquake (Ms 7.6) (Earthquake in website "Banglapedia"; Oldham, 1883; Ambraseys, 2004; Bilham and Hough, 2006 etc).   However, it seems that Bangladesh did not experience any large earthquake since 20th century for about 100 years.   The 1918 earthquake is thought not to be a characteristic one, since the magnitude is small for the plate boundary fault.   This may mean that Bangladesh has a high risk of large earthquake occurrence in near future.   Several major active faults, e.g. the plate boundary fault (the northern extension of subduction fault) and the Dauki Fault, are inferred in Bangladesh. These faults must generate large earthquakes over M 8.   However, the nature, detailed location, and the faulting history on these faults are not well known yet.

The trench investigation was carried out in 2008 for the first time as part of this project and the first report was drafted on January, 2009.   After then the report has been revised based on the TAG comments.   Additionally, the trench investigation for international expert of United Nations Development Programme (UNDP) was conducted.   Active faults in Bangladesh tend to be concealed due to thick unconsolidated Quaternary deposits and the fault topography is modified by severe cultivation and road construction.   This makes the trench investigation a difficult task.   However, the Dauki Fault was confirmed and the time of two seismic events on the activity of the Dauki Fault was revealed by trench investigation.   This will form the basis of future trench investigation and seismic hazard assessment in Bangladesh.

The results of both trench investigations above are contained in this report.

2. Tectonics, Seismicity and Historical Earthquakes

For the analysis of seismic source, tectonics, seismicity, and historical earthquakes are fundamental information.   First three items are described in this chapter based on the existing literatures.

2.1. Tectonics

The plate boundary between the Indian Plate and Eurasian Plate is shown in Figure 2-1. The Indian Plate is moving towards the north with slip rate of 6 cm/year, and subducting under the Eurasian Plate.   Large earthquakes were generated along the plate boundary under the compressive condition (Figure 2-2).   The subduction fault on the eastern edge of the Indian Plate is partitioned into two fault system, the northern extension of the subduction fault and the Sagaing Fault System for a right-lateral fault, from off Sumatra.

According to Yeats et al. (1997), the average slip rate of the Sagaing Fault is 6 cm/year and many historical earthquakes occurred along this fault (Figure 2-3).   However, the historical earthquake along the northern extension of the subduction fault is inferred to be only the 1762 event and the recurrence period is about 900 years (Shishikura et al., 2008, 2009). The recurrence period is too long for subduction fault.   Most of the strain along the plate boundary on the north of Sumatra may be consumed along the Sagaing Fault.

Shillong Plateau is located in the north of Bangladesh and the E-W trending Dauki Fault goes through on the southern fringe of Shillong Plateau (Figure 2-1).   The Dauki Fault may cross to the northern extension of the subduction fault in Sylhet.   However, the relationship between the Dauki Fault and plate boundary fault is not understood now.
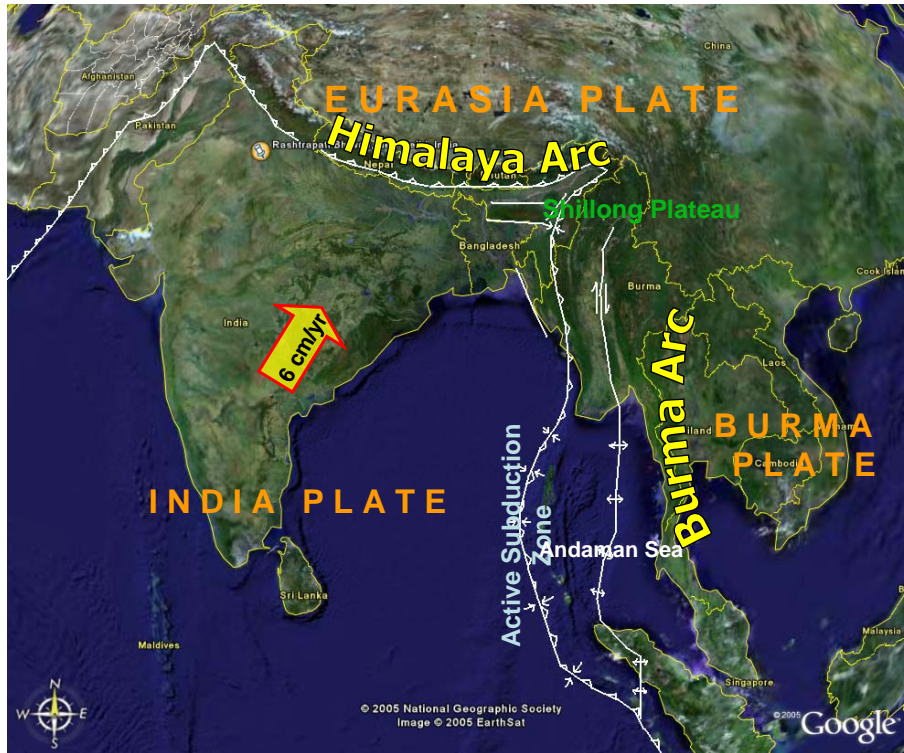
(Background: Google Earth)

Figure 2-1   Plate Boundary between Indian and Eurasian Plate

(Figure is offered with courtesy of Dr. S.H. Akhter.)
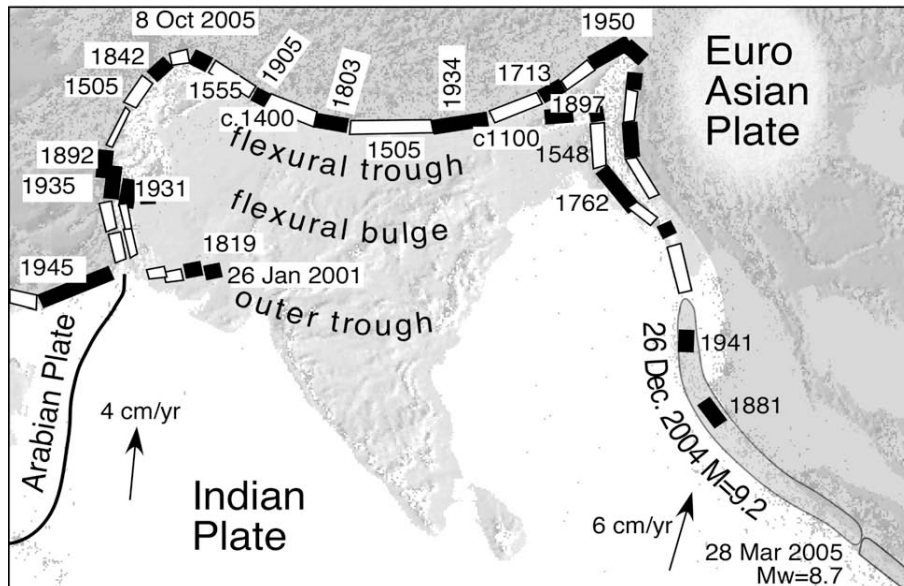
Figure 2-2   Historical Earthquakes along Indian and Eurasian Plate Boundary

(After Bilham and Hough, 2006)
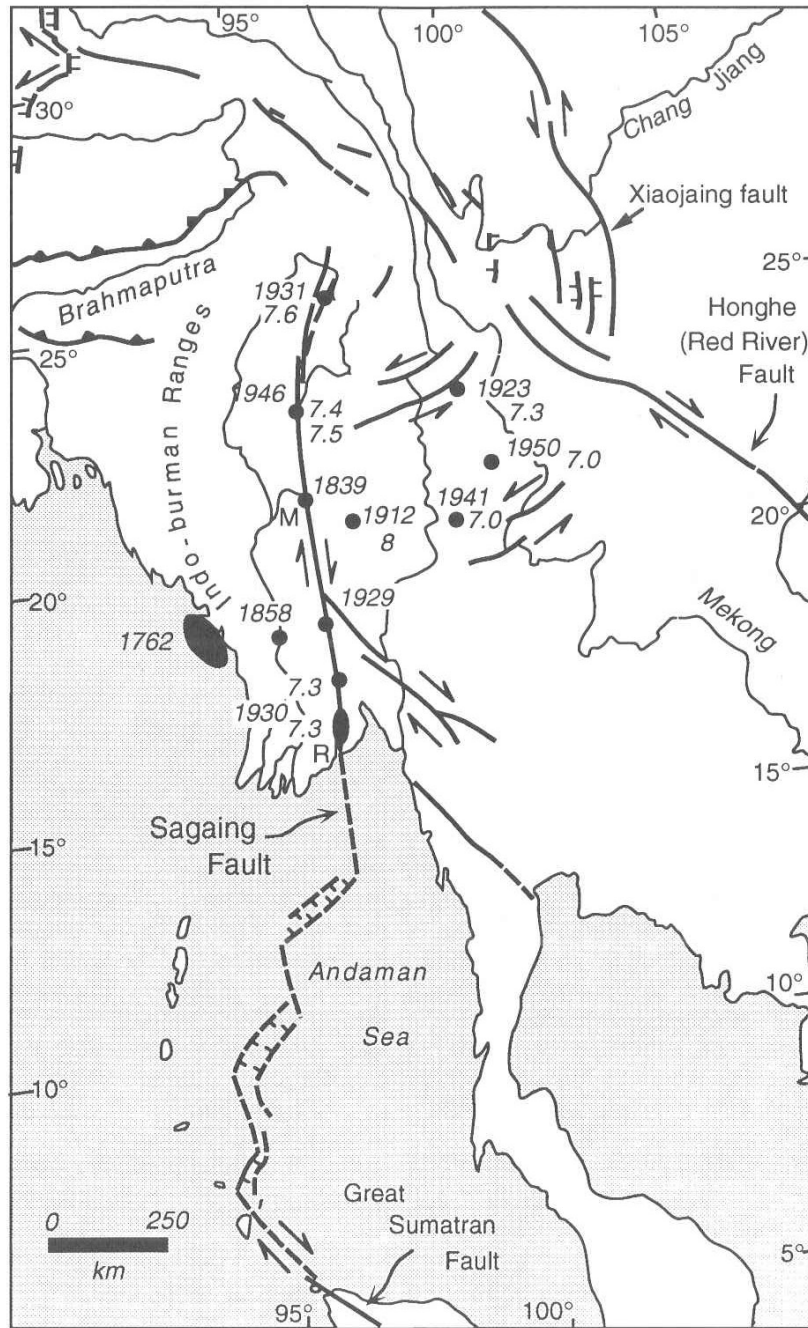
Figure 2-3 Sagaing Fault System and Historical Earthquakes along the Fault

(After Yeats et al., 1997)

2.2. Seismicity

Bangladesh has a couple of seismic networks such as network of BMD, BUET etc., but their history is short. Some Bangladeshi researchers have summarized seismicity data using the data of India and world observatory. Dr. M. A. Ansary of BUET kindly provided the recent catalogue from 1664 to present.

The seismicity classified in magnitude is shown in Figure 2-4. Figure 2-5 shows the seismicity classified in depth and historical earthquakes by Bilham (2004) are overlain on the seismicity. Figure 2-6 shows N-S and E-W cross section of the seismicity. As shown in these figures, the seismicity in Bangladesh is high along the plate boundary between the Indian and Eurasian Plate and the Dauki Fault.
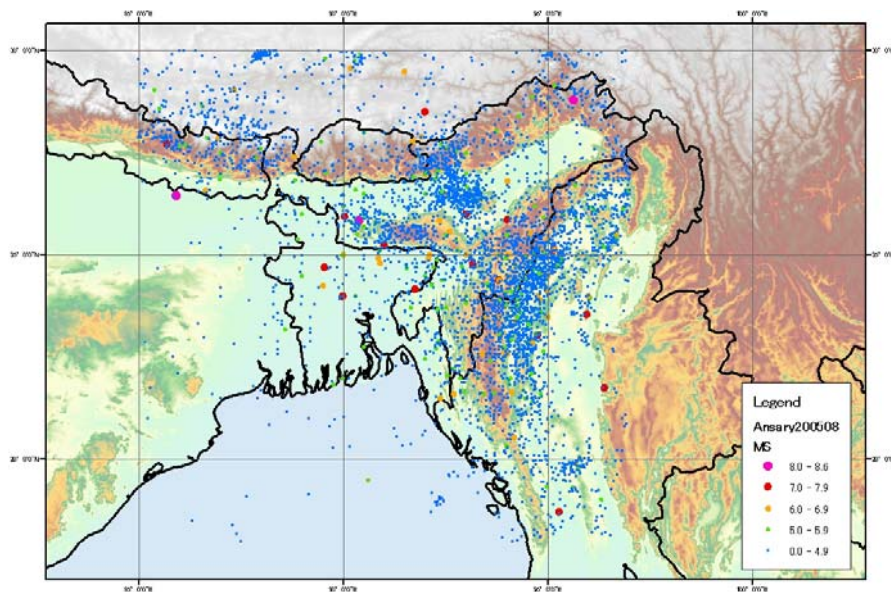
Figure 2-4　Seismicity classified in Magnitude in and around Bangladesh
(Data is offered with courtesy of Dr. M. A. Ansary.)
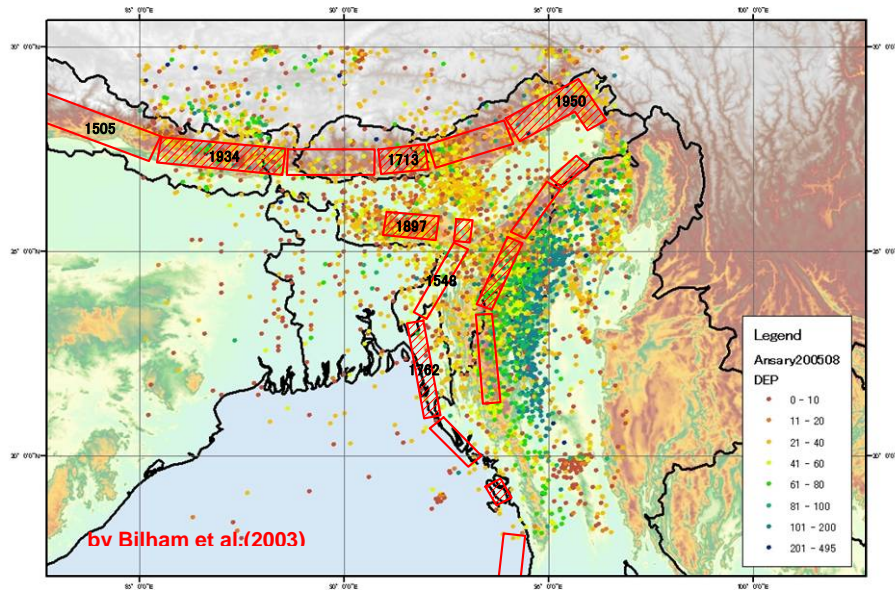
Figure 2-5   Seismicity classified in Depth and Source Region of Historical Earthquakes

(After Bilham, 2004)

Earthquake Catalogue: Prepared by Prof.Ansary, BUET
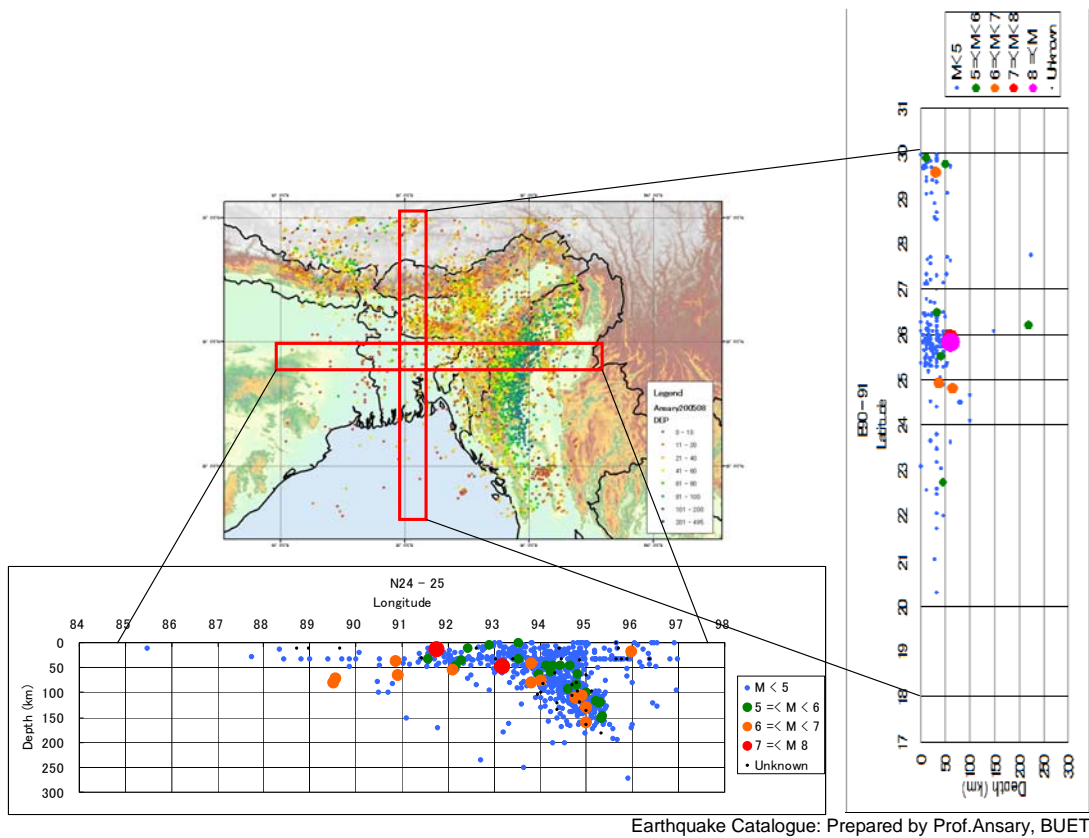
Figure 2-6   Cross Section of Seismicity

6

2.3. Historical Earthquake

Based on several earthquake catalogues, such as website "Banglapedia Earthquake", Sabri (2001), Utsu (2002) and Oldham (1883), the historical earthquakes in and around Bangladesh are shown in Table 2-1 and the epicenters are shown in Figure 2-7.

Table 2-1   List of Historical Earthquakes

No.	Year	Ms	Depth (km)	Source Area	Maximum MMI			
					Dhaka	Chittagong	Sylhet	Bangladesh
	1548?	?	?	Sylhet?				
	1664?	?	?	Shillong Plateau?				
	1762	?	?	Chittagong–Arakan	3?	8?	2?	8?
1	1858	6.5	?	Sandway, Myanmar	–	5?	–	6
2	1869	7.5	48	Cachar, India	5	4	8	8
3	1885	7.0	72	Sirajganj, Bangladesh	7	3	4	8
4	1897	8.1	60	Assam, India	8	6	8	9
5	1906	5.5	?	Calcutta, India	3	–	–	5
6	1912	7.9	25	Mandalay, Myanmar	?	2	?	?
7	1918	7.6	14	Srimangal, Bangladesh	5	5	7	8
8	1930	7.1	60	Dhubri, India	5	4	5	8
9	1934	8.3	33	Bihar, India–Nepal	?	?	?	?
10	1938	7.2	60	Mawlaik, Myanmar	–	5	–	5
11	1950	8.6	25	Assam, Himalaya	7	3	7	8
12	1954	7.4	180	Manipur, India	5	4	6	6
13	1975	6.7	112	Assam, India	4	3	5	6
14	1984	5.7	4	Cachar, India	–	–	3?	3
15	1988	6.6	65	Bihar, India–Nepal	–	–	–	–
16	1997	5.6	35	Sylhet, Bangladesh	5	3	6	7
17	1997	5.3	56	Bangladesh–Myanmar	4	6	3	7
18	1999	4.2	10	Maheskhali, Bangladesh	?	?	?	7

Ms and MMI are after Sabri (2001).

Blue: distant earthquakes from Bangladesh
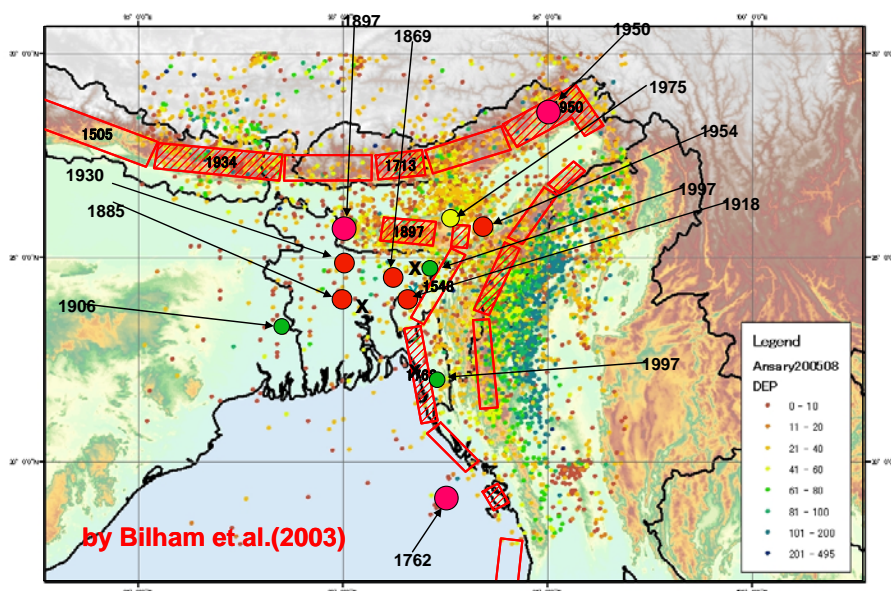
Figure 2-7   Epicenters of Historical Earthquakes (1664 – 2007)

(After Sabri, 2001)

7

The historical earthquakes that should be considered for the seismic source analysis are as follows;

(1)   1548 Earthquake

Sylhet and Chittagong suffered severe damage from this earthquake (website "Banglapedia Earthquake"; Bilham and Hough, 2006).   This earthquake occurred around Sylhet and may relate to one induced by the plate boundary on the eastern edge of Indian Plate.   However, detailed source region and damages are unknown.

As mentioned in the chapter of trench investigation, the latest event on the Dauki Fault corresponds with the 1897 Great Assam earthquake and the penultimate event may correspond with the 1548 earthquake.   The 1548 earthquake may have been generated by the activity of the Dauki Fault, not the plate boundary.

(2)   1664 Earthquake

According to Ambraseys (2004), an earthquake sometime between 1663 and 1664 caused considerable damages to Bangladesh.   The lake at the place, which is located on the north of Dhaka with seven days journey (about 140 km), has been dried up and new great lake appeared.   Most probably, this is the earthquake mentioned in contemporary diaries which sometime before 1676, damaged Chittagong and felt in Guwahati.   The source region may be beneath the Shillong Plateau.

(3)   1762 Earthquake

According to Oldham (1883), the region from Bengal to Arakan and Myanmar was strongly shaken.   Especially, the eastern coast of Bay of Bengal suffered severe damage.   In Dhaka, many persons lost their lives by tsunami (the death toll of 500 according to the website "Banglapedia Earthquake").   In Chittagong, a wide area was permanently subsided by liquefaction.   The western coast of Arakan and its surrounding islands were uplifted.   Shishikura et al. (2008, 2009) identified the marine terraces uplifted by this event in the islands of off Myanmar.   This event is noted as the earthquake that occurred on the northern extension of 2004 Mw 9.2 off Sumatra earthquake.

(4)   1869 Cachan Earthquake

In Sylhet, a strong tremor was felt, but there was no casualty (Figure 2-8).   The
magnitude is estimated to be Ms 7.5 (Sabri, 2001).

10 January 1869
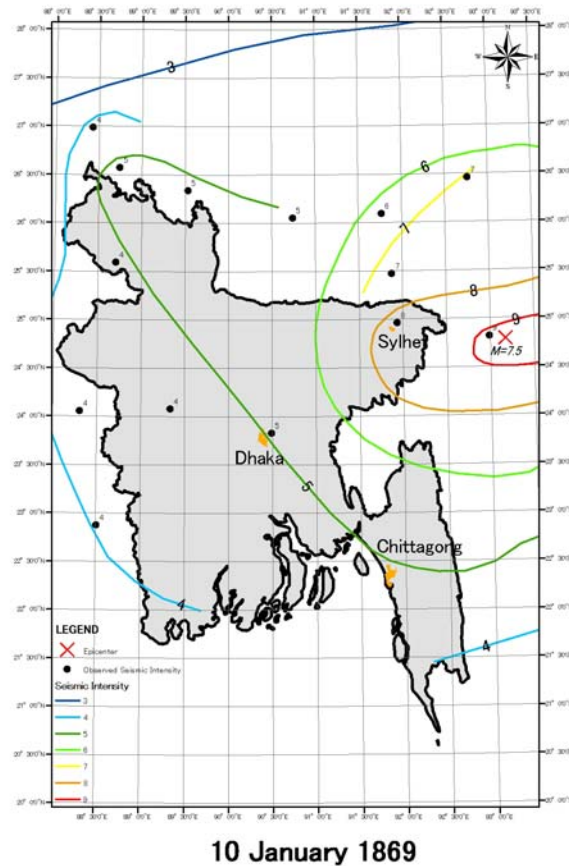
Figure 2-8   Seismic Intensity Distribution of the 1869 Earthquake
(After Sabri, 2001)

(5)   1885 Bengal Earthquake)

It is inferred that the epicenter of this earthquake is located on the northwest of
Dhaka (Figure 2-9) and this earthquake was generated by "deep-seated Jamuna
Fault" (website "Banglapedia Earthquake").   It seems reasonably that this
earthquake was generated by the activity of a blind fault.

14 July 1885
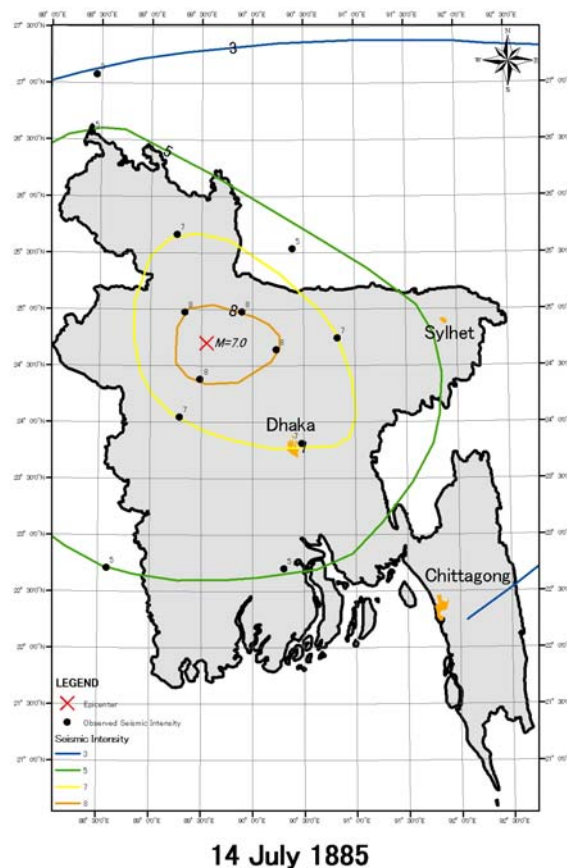
Figure 2-9　Seismic Intensity Distribution of the 1885 Earthquake
(After Sabri, 2001)

(6)　1897 Great India Earthquake

This event is known as the Great Assam Earthquake.　In Sylhet, the damage was severe and the death toll was 545.　In Mymensingh located on the north of Dhaka, the damage was large, but there was no casualty (Figure 2-10).　The magnitude is estimated to be Ms 8.0 by Bilham (2004) and Ms 8.7 by Sabri (2001).　Dauki Fault on the southern fringe of Shillong Plateau is suspected for the source of this earthquake.　However, there is no evidence for the ground surface rupture on the Dauki Fault (Yeats et al., 1997).　Bilham and England (2001) suggested that the source is a blind fault on the northern edge of Shillong Plateau.　The source of this earthquake is on debate internationally.　However, according the trench investigation at Gabrakhari site across the Dauki Fault, the source is inferred to be the Dauki Fault.

12 June 1897
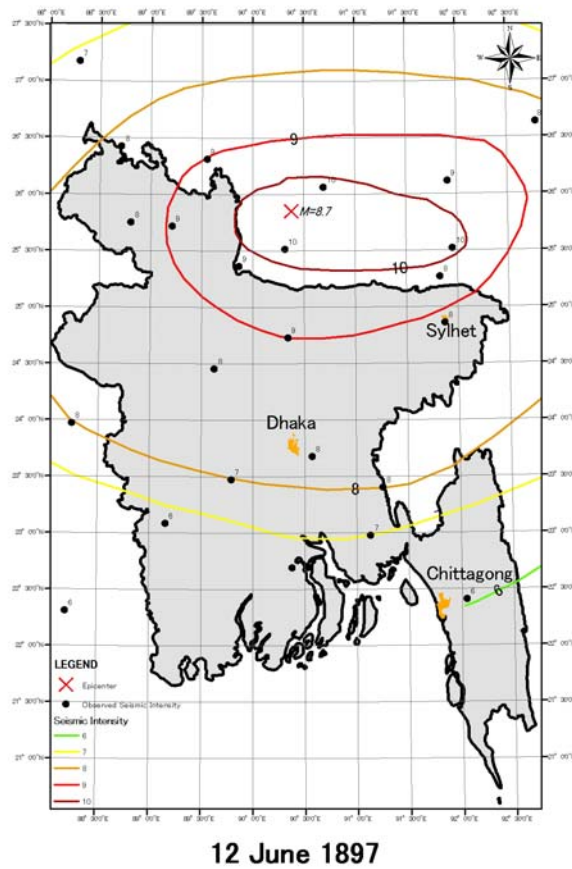
Figure 2-10   Seismic Intensity Distribution of the 1897 Great India Earthquake
(After Sabri, 2001)

(7)   1918 Srimangal Earthquake

This earthquake is notable for one that occurred around Sylhet (Figure 2-11).   The magnitude is estimated to be Ms 7.6 (Sabri, 2001).   The damage was reported around Srimangal located at 60 km south from Sylhet, while there was no damage in Sylhet and Dhaka.

11

08 July 1918
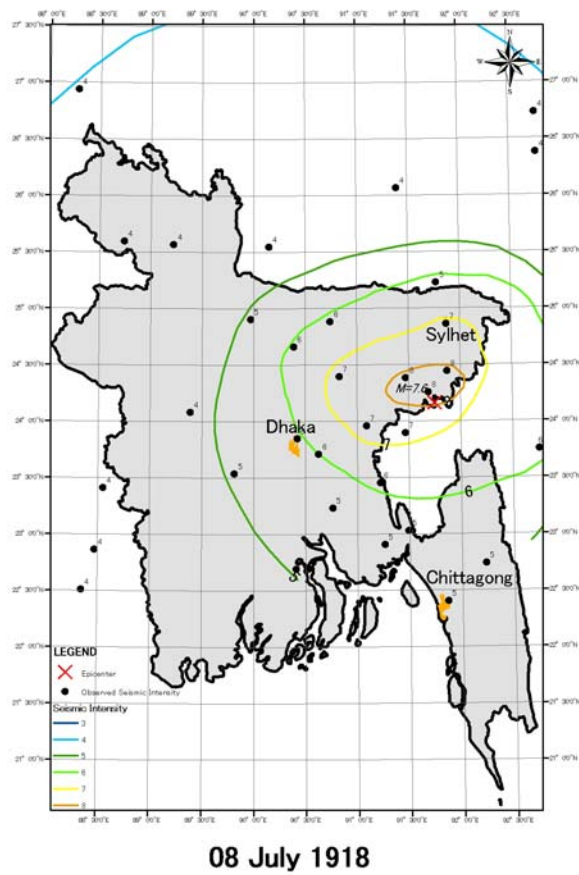
Figure 2-11   Seismic Intensity Distribution of the 1918 Srimangal Earthquake
(After Sabri, 2001)

3. Satellite Photo Interpretation and Field Survey

The CORONA photo was interpreted on almost whole Bangladesh and the locations of field survey were selected.   The field survey was carried out on the target area and the candidate sites of trench investigation were chosen.   The target areas of field survey are as follows: (1) Maheskhali, (2) Chittagong, (3) Feni, (4) Comilla, (5) Saetagonj, (6) northeast of Sylhet, (7) north of Chhatak, (8) Haluaghat, (9) northwest of Sherpur, (10) Madhupur, and (11) Saidpur (Figure 3-1).   The locations from (1) Maheskhali to (5) Saestagonj are targeted for the northern extension of the plate boundary fault.   The locations from (6) northeast of Sylhet to (9) northwest of Sherpur are targeted for the Dauki Fault.   (10) Madhupur is targeted for the Madhupur Fault, and (11) Saidpur is targeted for an active fault inferred by Nakata and Kumahara (2002).

Active fault is generally defined as one that ruptured repeatedly during the Late Quaternary and is capable of rupturing in future.   Active blind fault is included in active fault in the broad sense.   However, the blind fault does not accompany the displacement and deformation of the surface, therefore, can not be identified by the satellite photo interpretation. In this report, active fault is defined as one that reaches the surface and accompanies the displacement and deformation of the surface in the narrow sense.   If the fault does not reach the surface and is concealed near the surface, the fault must accompany the deformation such as warping scarp.   The concealed fault near the surface is regarded as active fault.

The fault topography such as low fault scarp, warping scarp, pressure ridge, and back-tilting surface etc. is created by paleo-earthquakes.   The geomorphic features of fault topography are estimated by satellite photo interpretation.   The blind fault which does not accompany the fault topography is not our target.   As a result of CORONA photo interpretation on almost whole Bangladesh, only the northern extension of the subduction fault, the Dauki Fault, and the active fault inferred in Saidpur are suggested to be active faults.

In Bangladesh, several active fault maps have been suggested so far.   However, any active fault maps have not referred to the fault topography inferred by satellite photo interpretation.   It is questionable how these active fault maps have been made.   The active fault map without satellite photo interpretation is unreliable.

Regarding to blind active faults detection, other types of investigation such as seismic reflection survey, drillings should be conducted in the future.
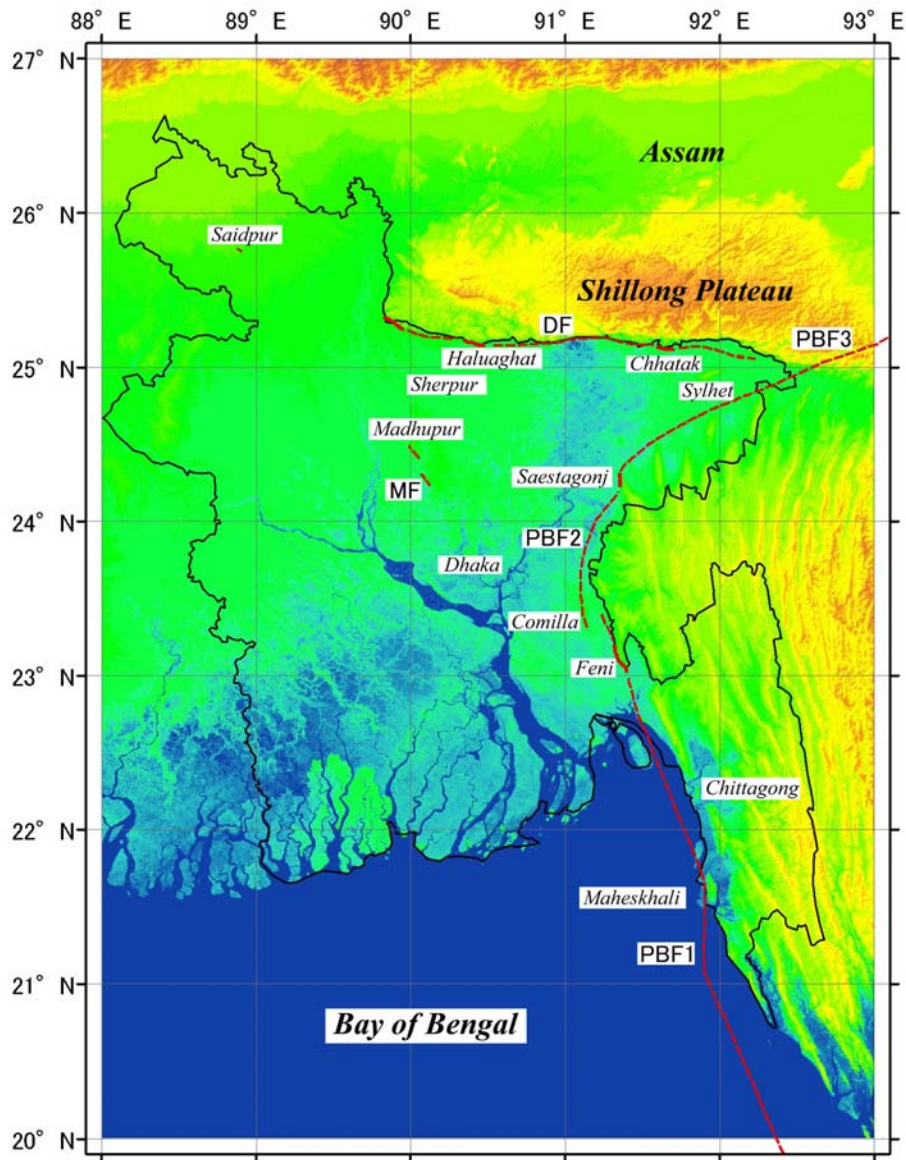
PBF1, PBF2, and PBF3: plate boundary fault

DF: Dauki Fault

MF: Madhupur Fault

Figure 3-1   Locations of Field Survey for the Active Fault Mapping

3.1. Maheskhali

The CORONA photo of Maheskhali is shown in Figure 3-2 and the enlarged photo for stereo-view in the south area of Maheskhali is shown in Figure 3-3. Three terraces T1, T2 and T3 are developed on the southern Maheskhali and a straight N-S trending low scarp was identified on the western edge of the terraces. This low scarp continues to the mouth of the small valley ('Al' as shown in Figure 3-3) located on the south of the terraces, and it is inferred to be a low fault scarp.

However, the low scarp could not be confirmed in the field, since a big dam was constructed on the western lowland and the low scarp was under water.

The fault inferred in Maheskhali may be another one that is developed on the hanging wall of the subduction fault.
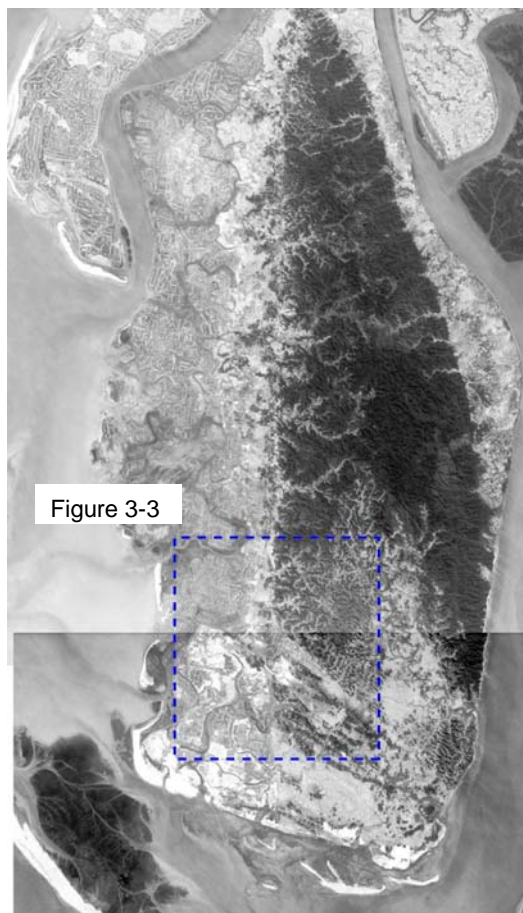
Figure 3-2   CORONA Photo of Maheskhali

T1, T2 and T3: terraces

Al: valley plain
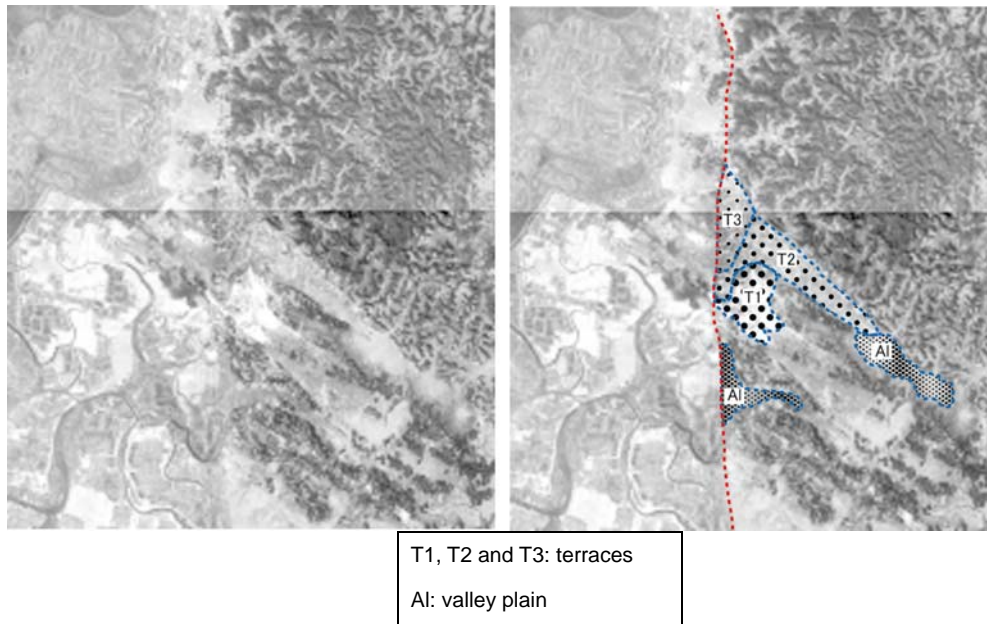
Figure 3-3   CORONA Photo for Stereo-View

3.2.   Chittagong

The CORONA photo of Chittagong and the enlarged photo of the topographic boundary between the hill and the alluvial plain are shown in Figure 3-4 and Figure 3-5, respectively. An active fault was suggested by the satellite photo interpretation along the arrow as shown in Figure 3-4.   However, a low fault scarp could not be confirmed in the field. The topographic boundary between the hill and the alluvial plain is much undulate and not straight, and the low scarps are not identified on the mouth of small valley.   If the ground surface was deformed by the 1762 earthquake, the low fault scarps must have been formed on the mouth of valley and be recognized on the CORONA photo.   The topographic boundary between the hill and the alluvial plain is inferred to be an eroded scarp.

The drilling data of GSB are shown in Figure 3-6.   The thickness of alluvium in Chittagong is shallow and the drillings reach Tertiary sedimentary rocks comprising of hills within 10 to 30 m in depth.   This indicates that Chittagong is located on the hanging wall of the subduction fault and the fault goes through off Chittagong.
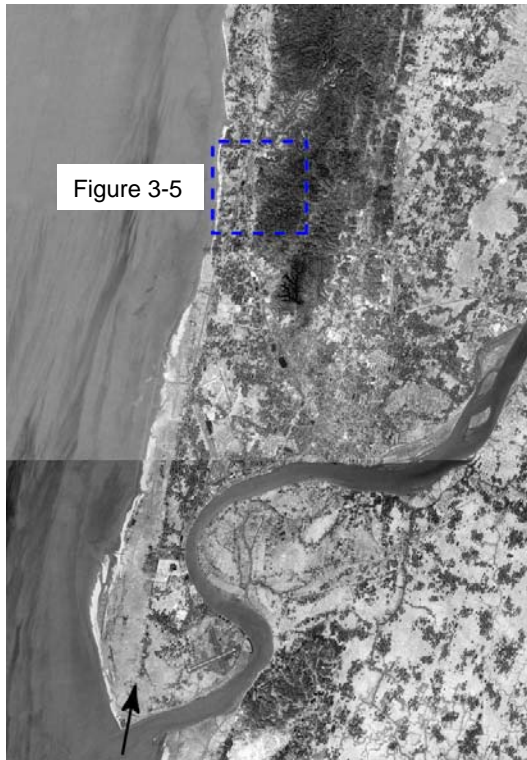
Figure 3-4   CORONA Photo of Chittagong
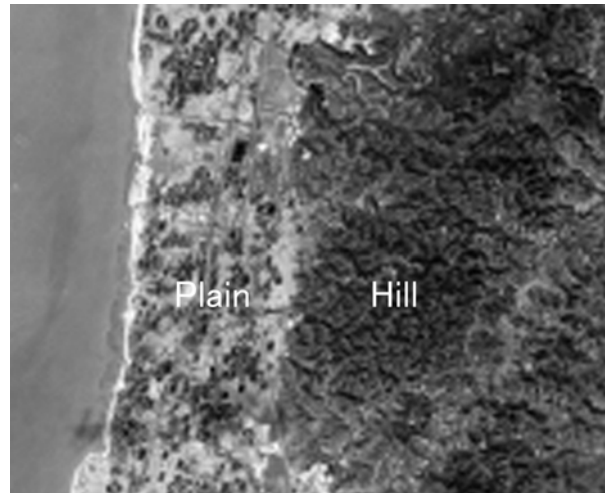
Figure 3-5   Enlarged CORONA Photo
(Location is shown in Figure 3-4)
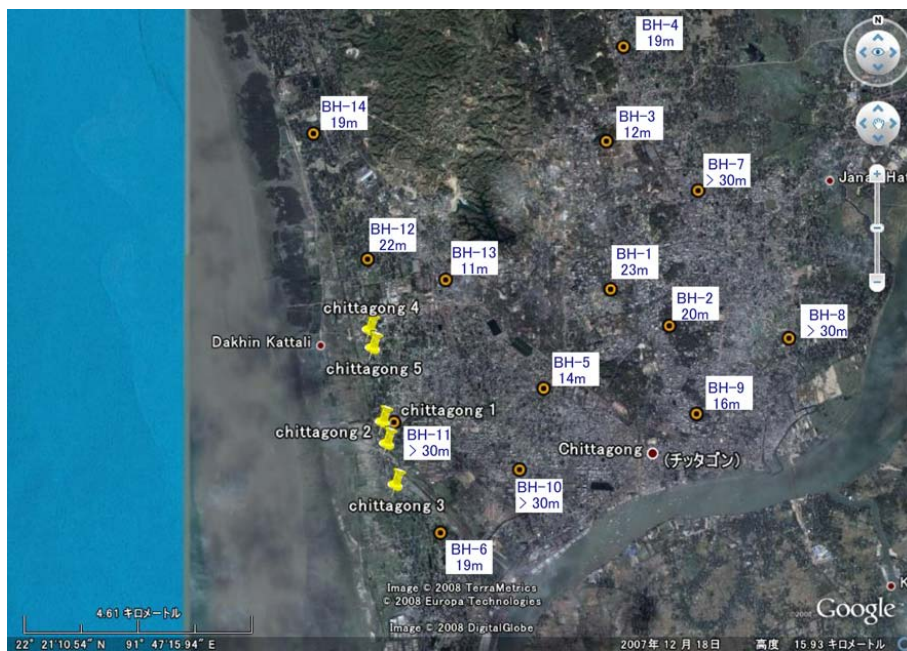
[The top and bottom in the rectangles represent the number of drilling and the depth of the top of the Tertiary sediments, respectively.   Data was offered with courtesy of GSB.]

Figure 3-6   Drilling Data in Chittagong

(Background: Google Earth)

17

3.3.   Feni

The narrow longitudinal N-S trending hill is recognized on the north of Feni (Figure 3-7).
The terrace and tableland are developed on the western fringe of the hill on the satellite photo.
According to existing geological map (Alam et al., 1990), the hill and tableland are composed
of the Tertiary sediments and the Pleistocene deposits (Dihing or Dupi Tila formation),
respectively.

The geomorphological map around location 7 to 9 is shown in Figure 3-8.   The terrace
is inferred to be uplifted alluvial plain and valley plain.   In this report, the uplifted alluvial
plain is called as uplifted terrace.   The low scarps are recognized on the topographic
boundary between the alluvial plain and the terrace or the tableland.   The low scarps are
inferred to be fault topography.   The low scarps are clearer on the topographic boundary
between the alluvial plain and the tableland, however, the low scarps between the alluvial
plain and the terrace is recognized at locations 7 and 8.   At location 8, the clear low scarp is
identified on the mouth of the broad valley.   Also the similar topography is observed at
location 7, however, the low scarp is modified by cultivation.

The low fault scarp located between hill and plane of northern Feni is inferred on the
basis of satellite photo interpretation.   However, it was difficult to carry out a detail and
satisfactory interpretation due to the presence of clouds in the photos.   Therefore, it was
planned to carry out a detail field survey at Feni to confirm the existence or inexistence of the
fault geography.

Figure 3-7   Location of Field Survey in Feni

(Background: Google Earth)
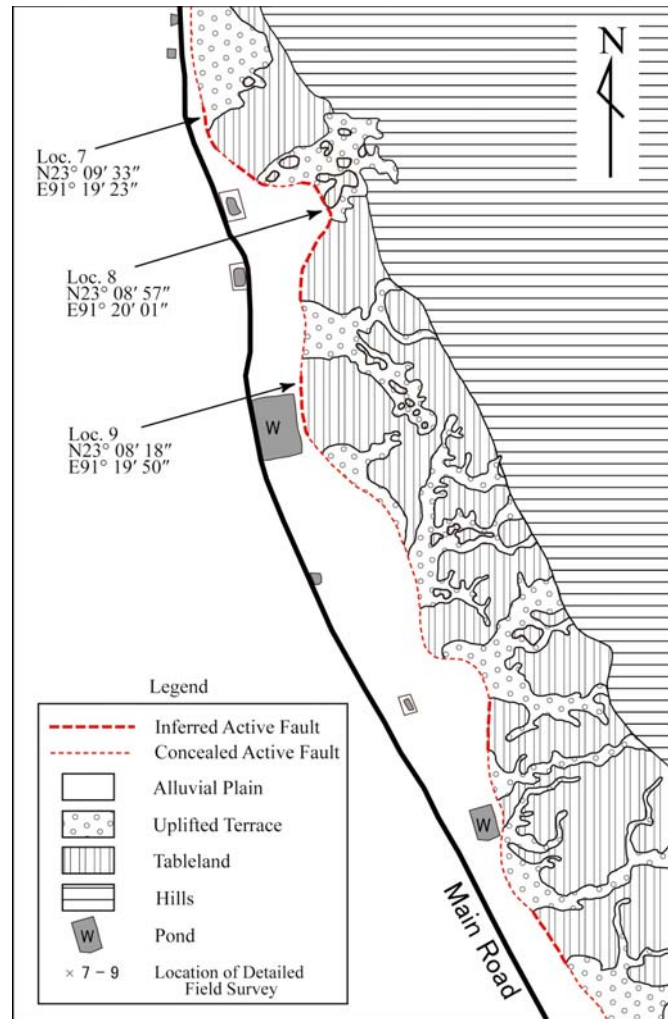
Figure 3-8   Geomorphology around Loc.7, Loc.8, and Loc.9 in Feni

The inferred active fault traces at locations 4 and 4-2, and location 4-3 are shown in Figure 3-9 and Figure 3-10, respectively.   The geomorphic features of uplifted terrace are clear at these locations.   As mentioned later, the trench investigation was carried out at locations 4-2 and 4-3.   However, the active fault did not reach the surface and only warping structure was confirmed in these trenches.   The active fault may be concealed near the surface in Feni.

Figure 3-9   Inferred Active Fault Trace in Loc.4 and Loc.4-2

(Background: Google Earth)

Figure 3-10   Inferred Active Fault Trace in Loc.4-3

(Background: Google Earth)

3.4. Comilla

The hill is developed on the west of Comilla (Figure 3-11).   According to the existing geological map, the active fault is inferred on the western edge of the hill.   However, the fault topography is not clear.   The terrace is recognized at the location of Comilla 2.   However, this terrace may be fluvial one, not uplifted one.   The low scarp on the western edge of the terrace may be an eroded one, since the low scarp on the western edge of the terrace is undulated (Figure 3-12).
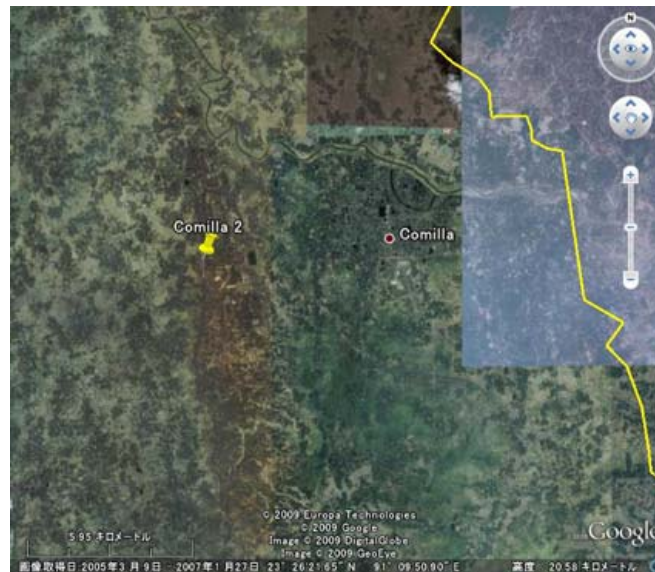
Figure 3-11   Location of Comilla 2

(Background: Google Earth)

Figure 3-12   Terrace on the Western Edge of Comilla 2

(Background: Google Earth)

3.5. Saestagonj

For the first satellite photo interpretation, the active fault was suggested to go through the topographic boundary between the hill and alluvial plain (Figure 3-13). However, the exposure of active fault and the geomorphic features indicative of active fault could not be confirmed in the field. The detailed satellite photo interpretation was performed and then a low warping scarp was identified in the alluvial plain about 500 m west from the topographic boundary (Figure 3-14). The low warping scarp is similar to the topography of the end of alluvial fan. However, the hill in Saestagonj is small in width and low in height, and the rivers flowing from the hill are also small. The hill can not form a broad fan shown in Figure 3-14. It is inferred that the flat land extended on the west of the hill is regarded as an uplifted terrace by the activity of the northern extension of the plate boundary fault, not an alluvial fan. The plate boundary fault in Saestagonj may be concealed just under the ground surface, since the warping scarp is very gentle and wide (width of arrows shown in Figure 3-14) with the height of 1-2 m.
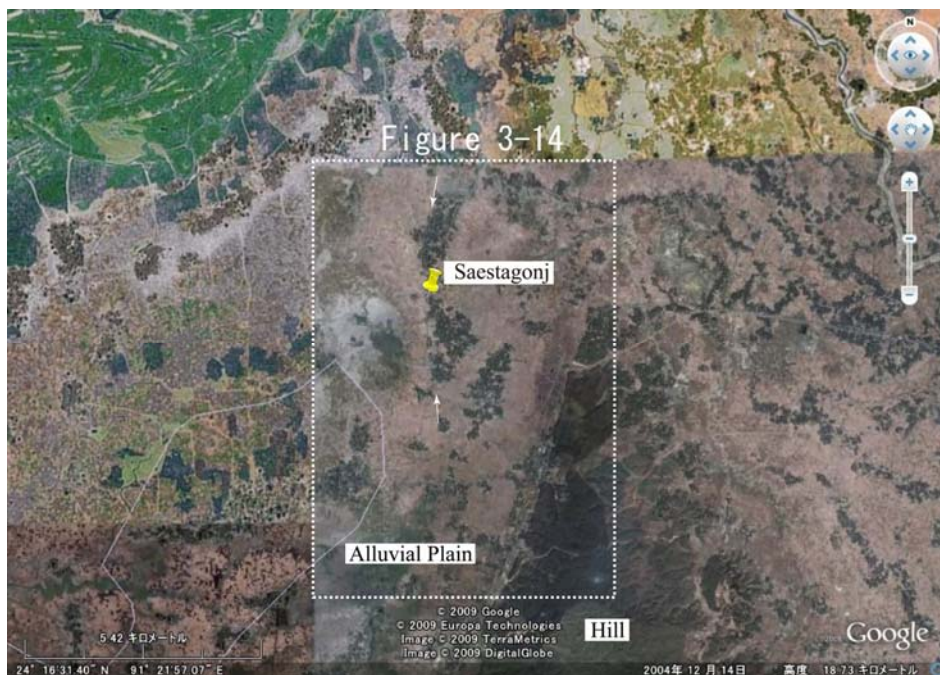
Figure 3-13 Location of Saestagonj

(Background: Google Earth)
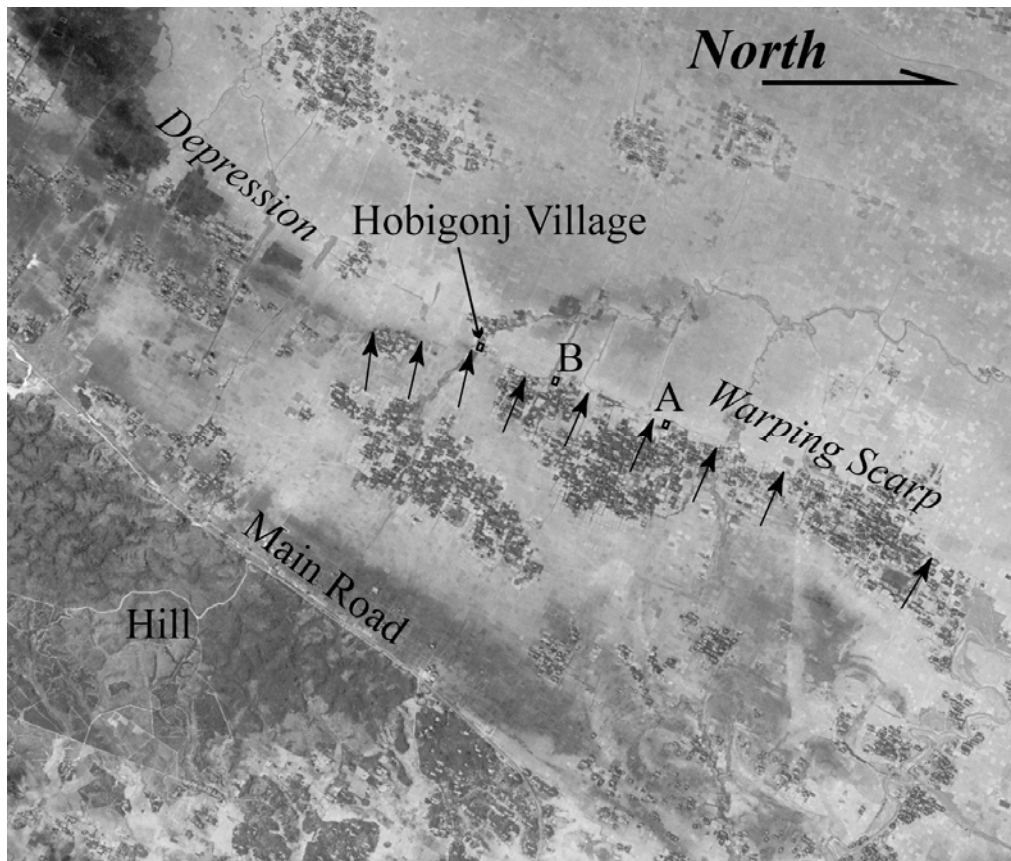
[Arrows represent warping scarp.   A and B are trench sites.   The crater as a paleo-liquefaction
was confirmed at Hobigonj Village.]

Figure 3-14   CORONA Photo Interpretation in Saestagonj

(Background: Google Earth)

3.6. Sylhet

Active fault traces were inferred on the northeast of Sylhet, the north of Chhatak, and near Sylhet airport (Figure 3-15).

Figure 3-15   Location of field Survey around Sylhet

(Background: Google Earth)

(1)   Northeast of Sylhet

The target area of northeast of Sylhet is located on the southern edge of the hills, which are extended to the south from Shillong Plateau (Figure 3-16) and the terrace was observed on the southern edge of the hills on the satellite photo.   A reverse fault generally shows foreland migration.   The E-W trending Dauki Fault inclined to the north may pass through on the southern edge of the terrace.   The terrace is inclined to the north.   This may be indicative of the deformation of the ground surface which was formed by the activity of the Dauki Fault.   The river with E-W direction is flowing along the low scarp on the southern edge of the terrace and bends towards the north in the west of the terrace.   This may be indicative of the uplift terrace.

However, the Dupi Tila Formation comprising the hill was recognized on the riverbed located in the south of the low scarp in the field. If the low scarp indicates an active fault, the footwall must be subsided and the younger Holocene deposits must be accumulated.   The Dauki Fault in this region may be concealed or go through more south.

[Arrows represent back-tilting surface]

Figure 3-16   Inferred Active Fault Trace in the Northeast of Sylhet

(Background: Google Earth)

(2)   North of Chhatak

According to satellite photo interpretation, E-W trending low warping scarps were identified on the side of alluvial fan (Figure 3-17).   Springs were inferred at the base of the low scarps and small channels are developed from the low scarps. Active fan is generally inclined to the downstream with gentle inclination.   Also springs are normally confirmed on the end of the fan.   The low scarps and springs on the side of the alluvial fan are indicative of the existence of an active fault.

Springs at two places were confirmed in the field.   However, the warping scarp was not confirmed.   The warping scarp may have been modified by cultivation.
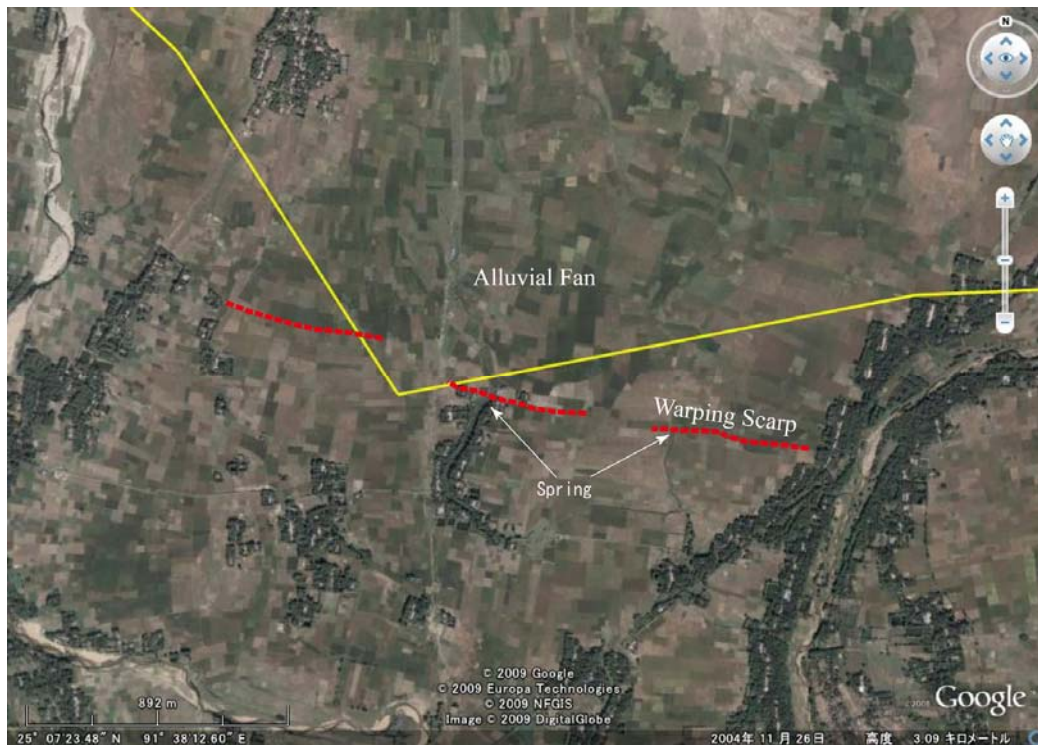
Figure 3-17   Inferred Active Fault Trace on the North of Chhatak

(Background: Google Earth)

(3)   Location near Sylhet airport

The hill located in the north of Sylhet Town, which is composed of Dihing or Dupi Tila formation, has a NE-SW trending spindle-shaped form.   This form is different from that of the hills extending to the north from Chittagong with N-S direction. Considering the form of the hill, the plate boundary fault is inferred on the northwestern edge of the hill.   The whole region around Sylhet was observed by satellite photo.   An active fault for the plate boundary is inferred only on the northwestern edge of the hill near Sylhet airport.   However, the fault topography and exposure indicative of active fault were not recognized in the field.   However, the hill is thought to be an important topography to understand the tectonics around Sylhet.   The detailed survey is necessary in future.

3.7.   Haluaghat

According to the CORONA photo interpretation, the Dauki Fault was inferred around Gabrakhari Village located in the north of Haluaghat (Figure 3-18).   The narrow terrace is developed on the southern edge of the hills.   The terrace is uplifted alluvial plain and an

26

active fault is inferred on the topographic boundary between the alluvial plain and the terrace. The whitish part shown in Figure 3-18 represents uplifted terrace. According to the field survey, the fault topography is clearest in the region shown in Figure 3-19. However, this region is located near the border and the detailed field survey could not be carried out. Therefore, the east of this region was surveyed and the back-tilting terrace surface was found out (Figure 3-20 and Figure 3-21).

The fluvial terrace is generally inclined to the downstream. The fluvial terrace around Gabrakhari Village should be inclined to the south, since the rivers flow from north to south. As shown in Figure 3-21, the terrace is inclined towards the north at Gabrakhari 1 site. This terrace is inferred to be the uplifted terrace, not fluvial terrace. This geomorphology is called as back-tilting terrace surface for technical term. The back-tilting terrace is also confirmed in the west of Gabrakhari 1 site. The height of the uplifted terrace on the alluvial plain is 2.25 m (Figure 3-21).
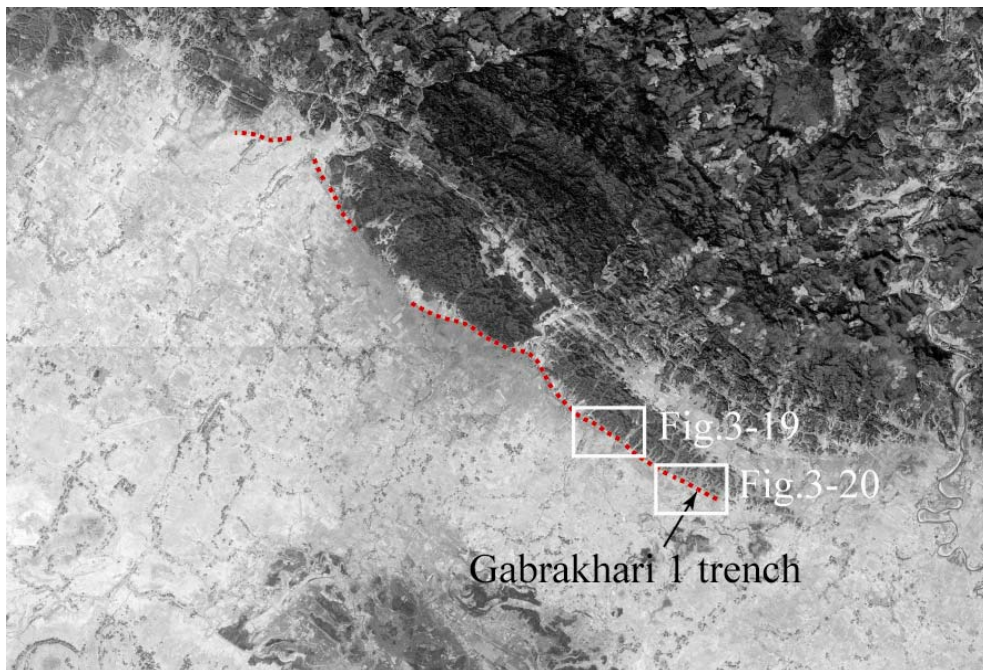
Figure 3-18 Inferred Active Fault in the North of Haluaghat
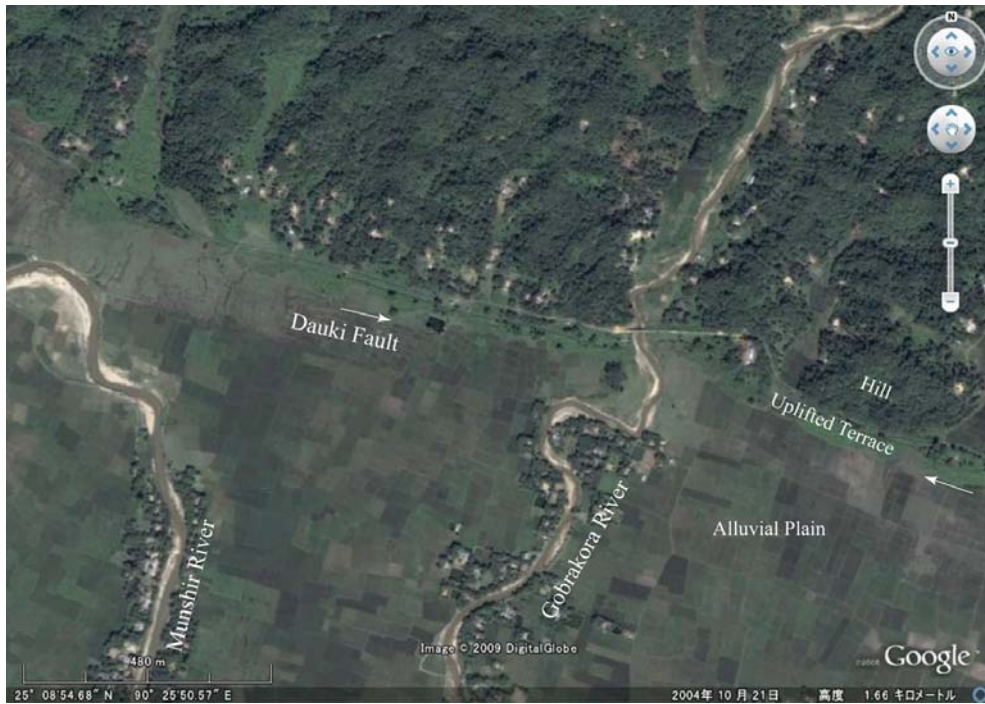
Figure 3-19   Active Fault in the West of Gabrakhari

(Background: Google Earth)
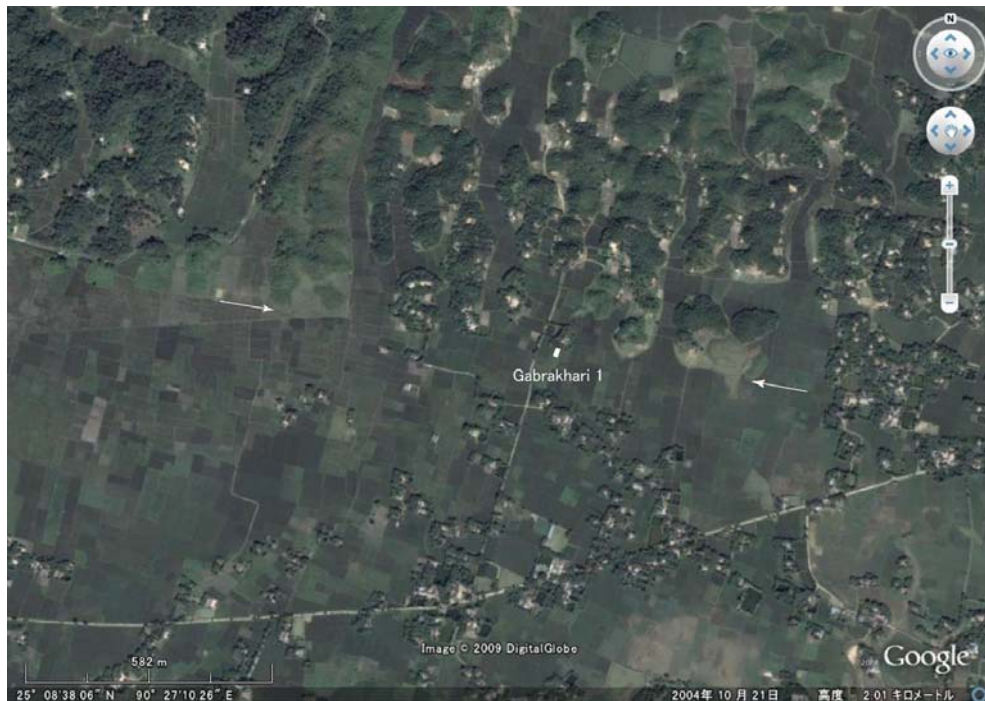
Figure 3-20   Active Fault at the Trench Site of Gabrakhari 1

(Background: Google Earth)
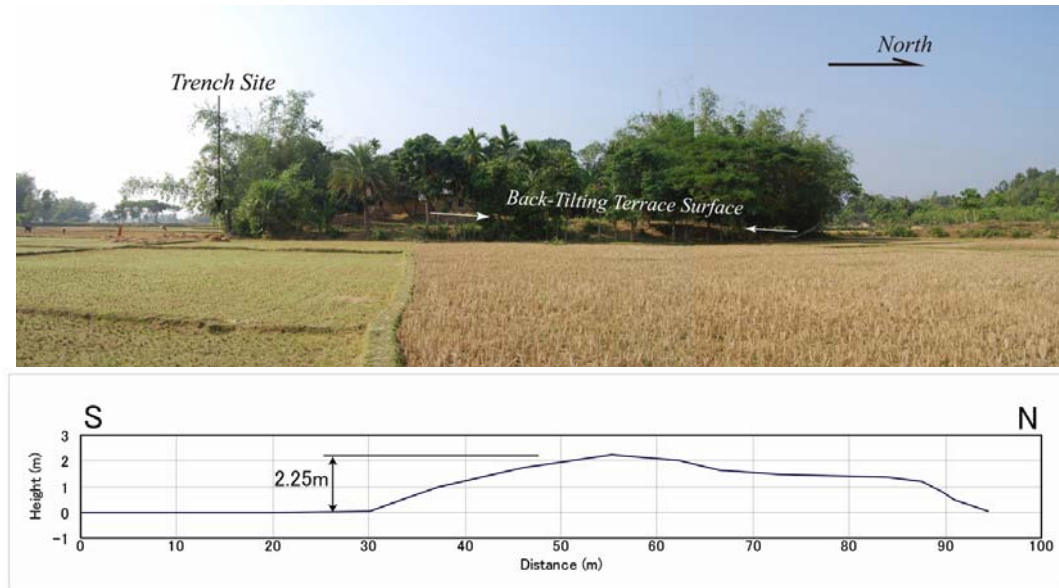
Figure 3-21   Photo of Back-Tilting Terrace Surface at Gabrakhari 1 Trench Site (Top) and the Topographic Profile (Bottom)

3.8.   Northwest of Sherpur

The Dauki Fault was inferred in the northwest of Sherpur on the CORONA photo (Figure 3-1 and Figure 3-22).   The narrow terrace is identified on the north of the low scarp like Gabrakhari Village.   However, the low scarp may be eroded one, since Jamuna River flow near this region.   The detailed field survey was not carried out, since this region is located near the border.
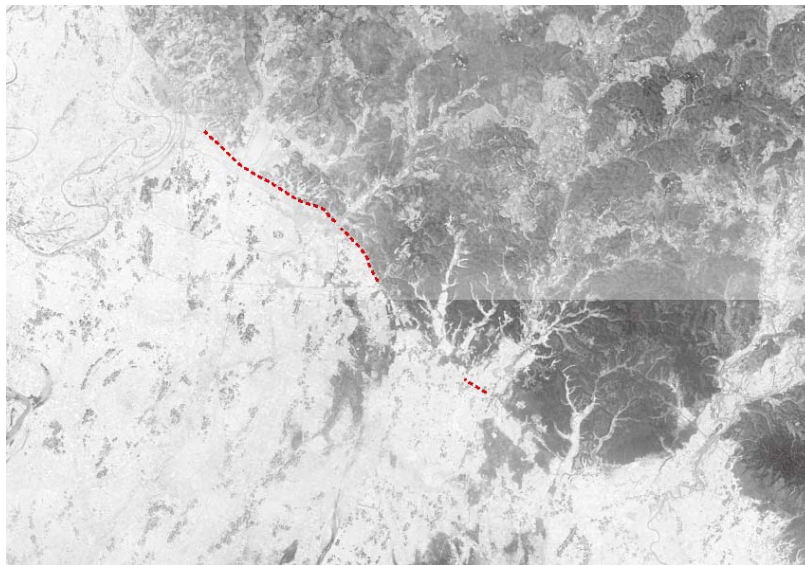
Figure 3-22   Inferred Active Fault on the Northwest of Sherpur

3.9. Madhupur

The satellite photo of Madhupur and the enlarged photo are shown in Figure 3-23 and Figure 3-24, respectively. The straight NNW-SSE trending low scarp was identified on the western edge of Madhupur block on the CORONA photo. However, the low scarp is inferred to be eroded one, since the scarp is too straight, any uplifted terrace is not confirmed on the western edge of the Madhupur block, and a low scarp is not identified on the mouth of the small valley ("A" shown in Figure 3-24). However, Madhupur block is surely uplifted and inclined towards the east. Furthermore, the Late Pleistocene deposits (Madhupur Formation) are exposed on the surface. The low fault scarp on the western edge of the Madhupur block must have been eroded, if an active fault is present.
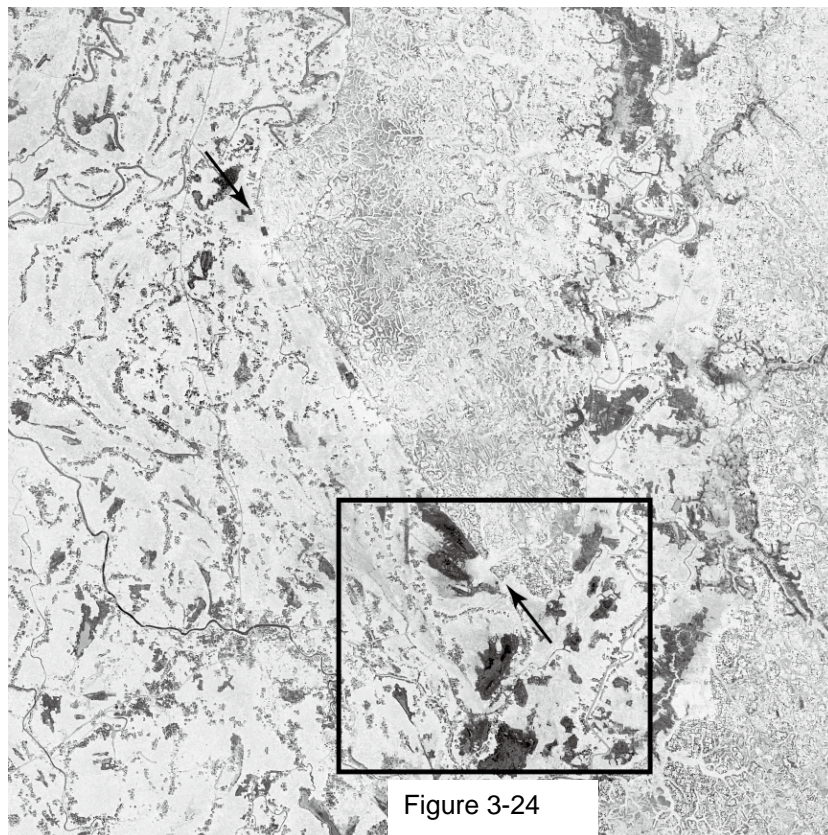
Figure 3-23 CORONA Photo of Madhupur
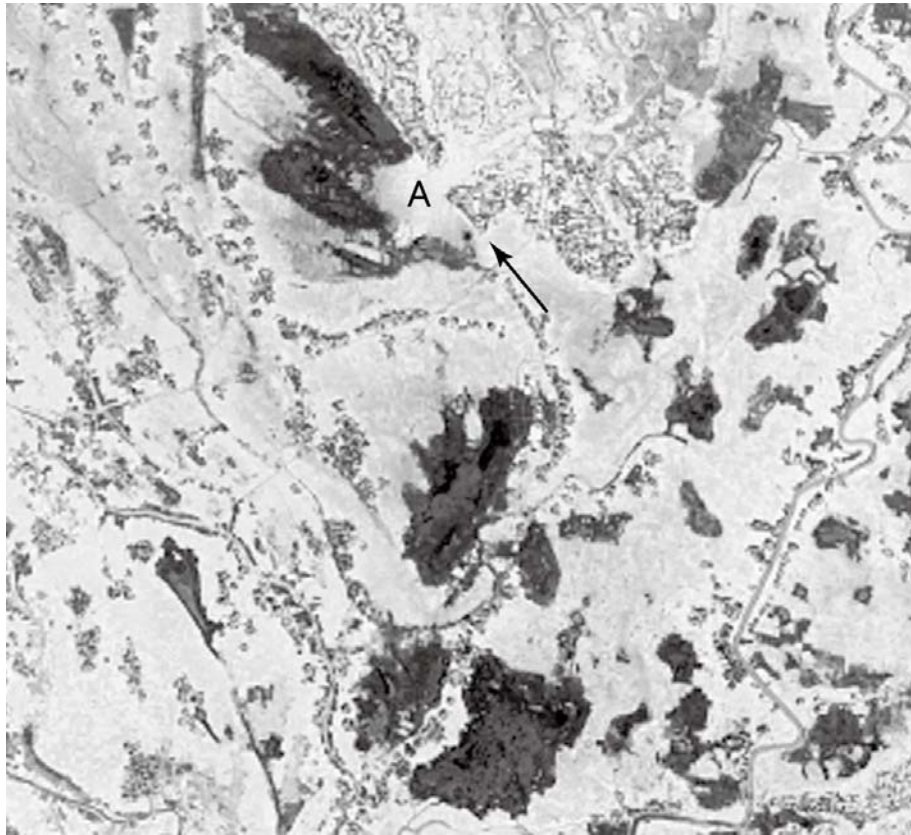
Figure 3-24   Close-View of CORONA Photo
(The location is shown in Figure 3-23.)

3.10. Saidpur

Nakata and Kumahara (2002) suggested a right-lateral fault extending from Kakarbitta in Nepal to Saidpur in the northwest of Bangladesh.   According to the CORONA photo interpretation, the low scarp is developed in the southwest of Saidpur Town (Figure 3-25). The height of the scarp is 1-2 m and the low scarp shows a warped shape with cross section like a warping scarp.   However, the scarp may be eroded, since the river flows along the scarp.

As mentioned in the chapter of trench investigation, the fault could not be confirmed, since the trench excavation was difficult due to rice cultivation.   Further detailed investigation shall be conducted.
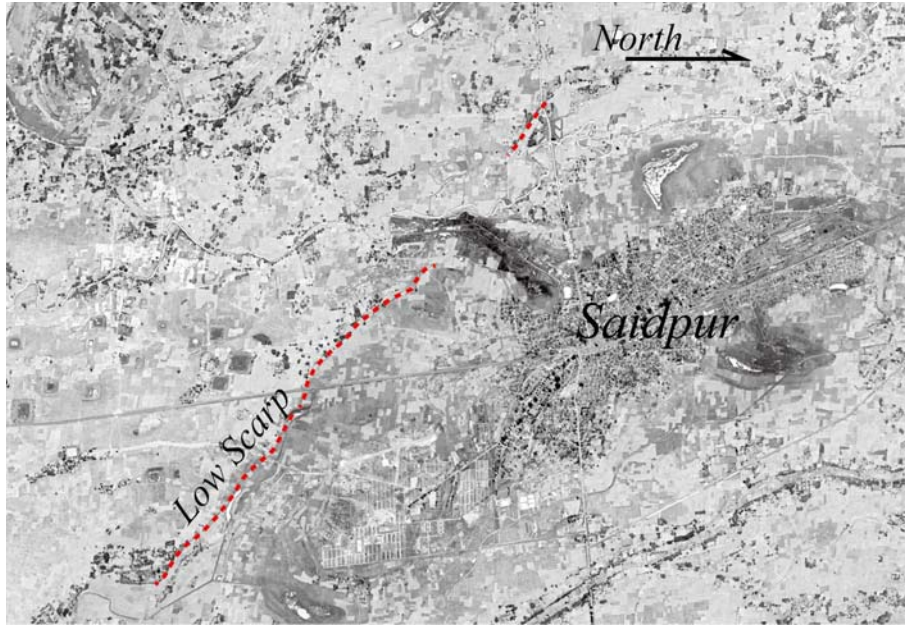
Figure 3-25   Inferred Active Fault in Saidpur

4. Trench Investigation

After the satellite photo interpretation and field survey, some candidates for active faults were selected. For this context, the trench investigation in Haluaghat, Feni, Saetagonj, and Saidpur was carried out (see Figure 3-1). In Saidpur, small trench (pilot trench) was excavated, since the rice before harvest was planted at the trench site. More trench investigation is necessary in Saidpur on December to January when rice is not planted.

4.1. Trench Investigation across the Dauki Fault at Gabrakhari Village, Haluaghat

The location of trench sites at Gabrakhari Village is shown in Figure 4-1. Four trenches were excavated at Gabrakhari, however, an active fault was identified only at Gabrakhari 1 trench site. The gentle warping structure was recognized at Gabrakhari 2 trench site. Paleo-liquefaction was found out at Awlatory Village. In this chapter, the trench investigation at the sites of Gabrakhari 1 and 2, and the paleo-liquefaction at Awlatory are described.
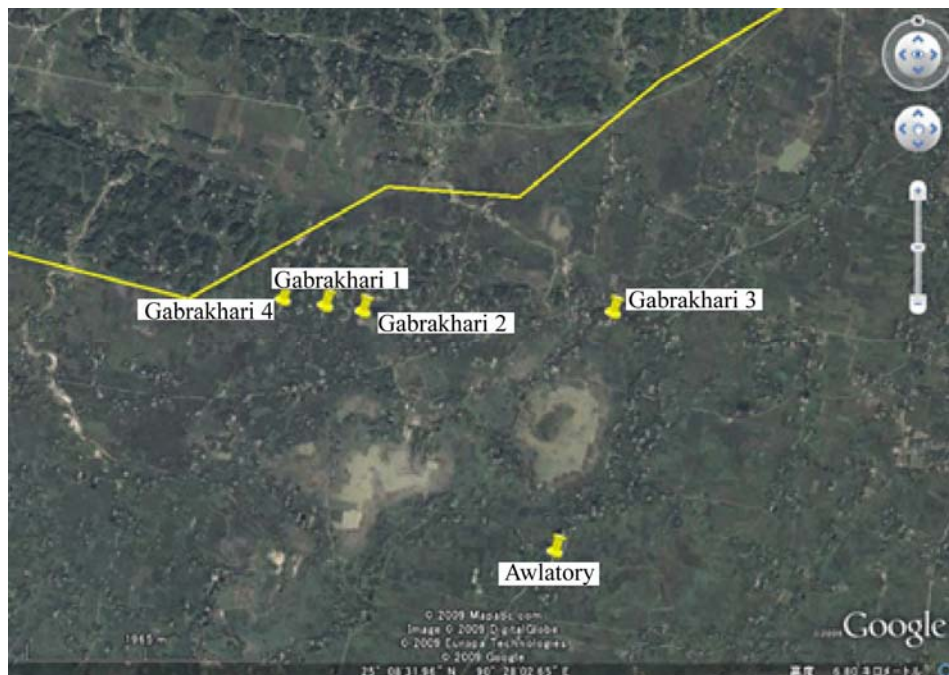
Figure 4-1   Location of Trench Sites at Gabrakhari Village, Haluaghat, Mymensingh

(Background: Google Earth)

4.1.1.   Trench Investigation at Gabrakhari 1 Site

As mentioned in the Chapter 3, the back-tilting terrace surface was recognized at Gabrakhari site.   The trench at Gabrakhari 1 site was excavated on the southern edge of the terrace, since the back-tilting of the terrace surface is created by the activity of the Dauki Fault.

(1)   Stratigraphy identified in the Gabbrakhari 1 Trench

10 m long, 5 m wide, 2 to 2.5 m deep trench was excavated.   The log and mosaic photo of the west wall are shown in Figure 4-2 and Figure 4-3.   The result of ^{14}C dating is shown in Table 4-1.

The exposed sedimentary succession in the trench is divided into unit A to I and a number of sand dikes due to liquefaction are identified in the trench.

Unit A: Reddish-brown sandy clay

This unit covers the sand dikes which intruded to the top of unit B.   The ^{14}C dating of two samples shows older age than lower units.   This unit may be artificial soil.

Unit B: Yellowish-brown medium sand

The ^{14}C dating of two samples shows older date as unit A.   This unit also may be artificial soil.

Unit C: Reddish-brown medium sand

The fragments of unglazed pottery were identified in this unit.   The unit between W2 and W5 horizontal markers is waved and seems to be deformed by the shaking of the earthquake.   The unit between W1 and W5 is gently inclined towards the south.   This may be indicative of warping structure deformed by the activity of the Dauki Fault.   The radiocarbon age of the charcoal contained in this unit shows 70 ± 40 yBP (Cal AD1700 to 1960). "yBP" is an abbreviation of "years before present (1950)" which represents conventional radiocarbon age.   "Cal" is an abbreviation of "calibration" which means the calibration of radiocarbon age to calendar years.

Unit D: Yellowish-blown fine to medium sand

The fragments of unglazed pottery are identified in this unit.   The sand dikes are intruded horizontally along the stratigraphic boundary between units D and E, therefore, the unit boundary between units D and E is obscure. The radiocarbon age of this unit shows 50 ± 40 yBP (Cal AD 1890 to 1960). The unit between W0 and W5 horizontal markers is inclined towards the south and shows warping structure.

Unit E: Silt and fine sand

> This unit is inferred to be sag pond deposits because the size of the materials is fine grained. The sand dikes intrude into the unit as sills, and the structure is disturbed. The radiocarbon ages show 120 ± 40 yBP (Cal AD1680 to 1960) and 160 ± 40 yBP (Cal AD 1670 to 1950).

Unit F: Alternation of fine sand and silt

> This unit is inferred to be sag pond deposits.   The unit between W2 and W5 is inclined towards the south with the inclination of 10°, however, shows horizontal structure between W6 and W10.   This means warping structure. The radiocarbon ages show 200 ± 40 yBP (Cal AD1660 to 1950) and 310 ± 40 yBP (Cal AD 1500 to 1660).

Unit G: Blue peaty clay

> The unit is inferred to be marsh deposits.   The lower to middle part of the unit is displaced by the fault.   However, the upper part of the unit is not shifted and shows only deformation inclined towards the south with the inclination of 30° to 40°.   The radiocarbon ages shows 330 ± 40 yBP (Cal AD 1480 to 1640) and 360 ± 40 yBP (Cal AD 1460 to 1630).

Units H and I: Gravel comprising the terrace

> These units are fluvial deposits containing pebbles of chert etc. which were provided from Shillong Plateau.   The units are divided into unit H and I by the content of gravel.   Unit H contains much gravel than unit I.

Sand dike:

> The sand dikes in unit E are composed of coarse to medium sand and those on the upper part shows fine to medium sand.   The upward fining of grain size is recognized.

(2)   Fault and Warping Structure identified in the Gabrakhari 1 Trench

Units E and F between W3 and W6 horizontal markers are inclined towards the south with the inclination of about 10° and those between W6 and W10 are horizontal.   Units B, C, and D between W1 and W5 are also gently inclined towards the south. T he inclination to the south represents warping structure.   The top of unit H is inclined towards the south with the inclination of 20° which is twice steeper than that of units E and F.   This possibly indicates that unit H is deformed twice by the activity of Dauki Fault.

The sand dikes reach the top of unit B and is covered by unit A on the west wall (Figure 4-2).   The stratigraphic relationship between the sand dike and the layer is

clearer on the east wall (Figure 4-7 and Figure 4-8). The latest event occurred after the deposition of unit B and before the deposition of unit A.

The fault was identified near the bottom of the trench around W4 horizontal marker (Figure 4-4 and Figure 4-5). The fault displaces units G, H, and I, however, dies out in the upper part of unit G. The trench was excavated deeper just before the closing the trench (Figure 4-4 and Figure 4-6). A couple of small faults displacing units G and H were identified clearer, and it was confirmed that unit G near the fault is steeply inclined towards the south and covered by unit F with unconformity. It is evident that the penultimate event occurred after the deposition of unit G and before the deposition of unit F.

(3)   Environment of Deposition

Unit G is peaty clay. The trench site was under the environment of marsh during the deposition of unit G. Then the environment had changed into sag pond, and units F and E had been deposited. As above-mentioned, units E and F covered unit G with unconformity. The land around the trench site was subsided by the activity of the Daulki Fault and the environment may have been suddenly changed from marsh to sag pond. The fragments of unglazed pottery are recognized in units D and C. The agriculture around the trench site started from the time of the deposition of unit D. Units B and C may be artificial soil. After the deposition of unit B, a large earthquake occurred, and sand dikes induced by liquefaction intruded to the upper layers and reached to the top of unit B. Next, unit A covered the sand dikes.

(4)   Time of Paleo-Earthquakes

Latest event

Units C to F show warping structure. The sand dikes due to liquefaction reach the top of unit B and are covered by unit A. The latest event occurred after the deposition of unit B and before the deposition of unit A. The radiocarbon age of unit D shows AD 1700 to 1960. The historical earthquake which corresponds with the latest event along the Dauki Fault is only the 1897 Great Assam Earthquake.

Penultimate Event

Unit G is highly deformed and is covered by unit F in relation to unconformity. The penultimate event occurred after the deposition of unit G and before the deposition of unit F. According to the radiocarbon age of units F and G, the time of the penultimate event is inferred to be AD 1500 to 1630. Either of the 1548

earthquake and the 1664 earthquake is the candidate of this event. However, the radiocarbon ages of unit G and F indicates the 1548 earthquake for the penultimate event along the Dauki Fault.

Figure 4-2   Log of the West Wall of Gabrakhari 1 Trench
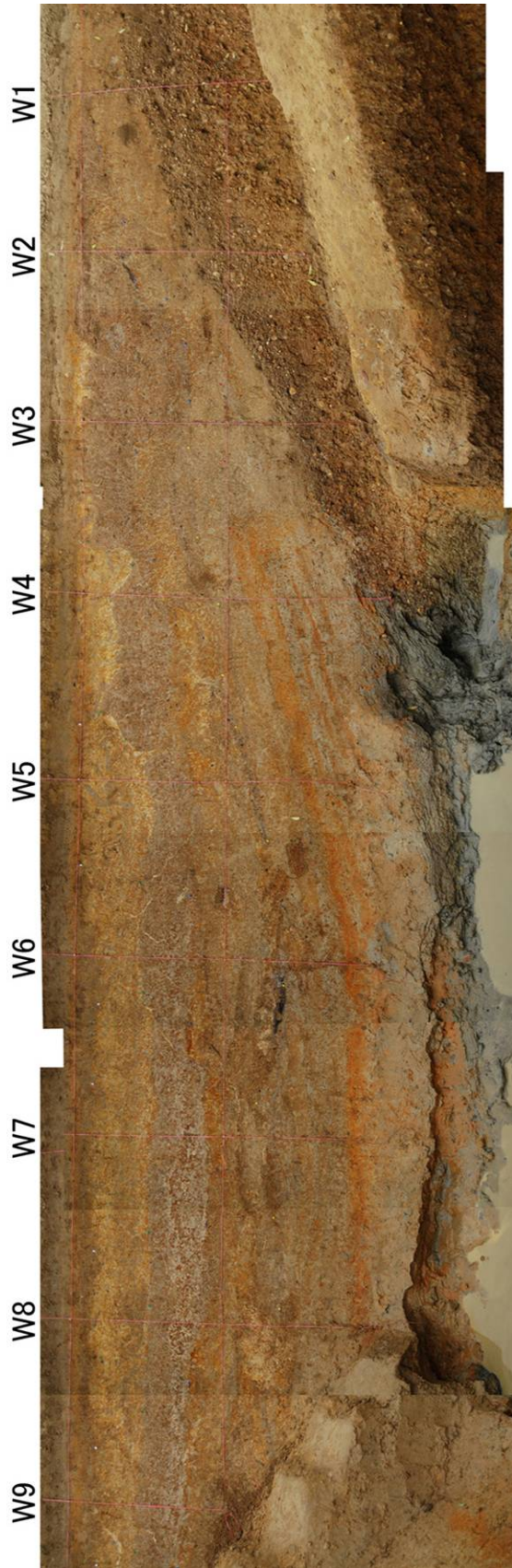
Figure 4-3   Mosaic Photo of the West Wall of Gabrakhari 1 Trench
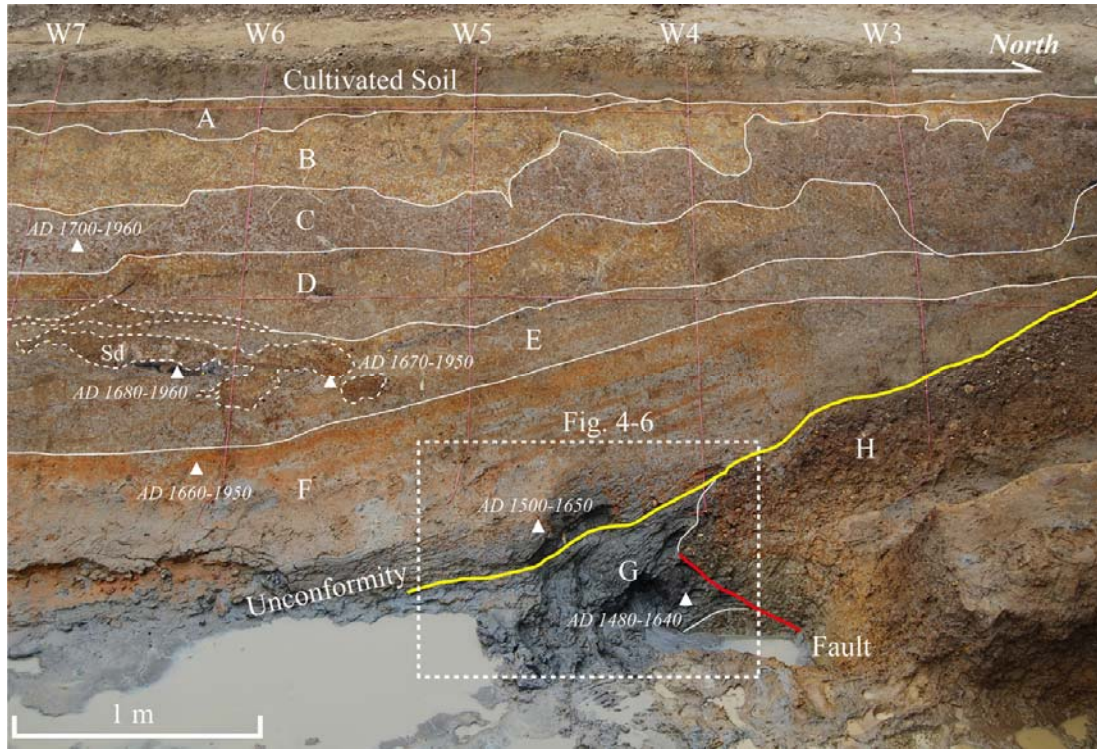
Figure 4-4   Photo of the West Wall

Figure 4-5   Close-View of the Fault
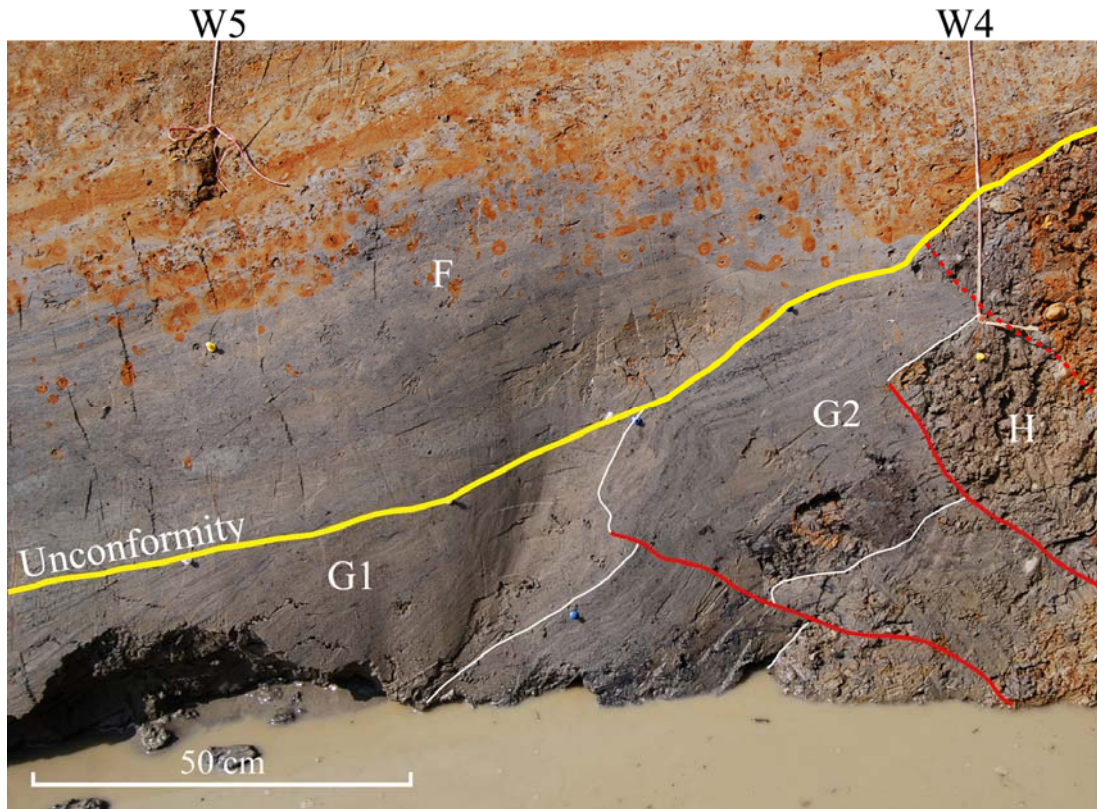
[Unit G is divided into subunits G1 and G2. A couple of small faults displacing units G and H were identified clearer, and unit G near the fault is steeply inclined towards the south. Unit F covers unit G with unconformity.]

Figure 4-6 Close-View of the broken Rectangle Part of Figure 4-4
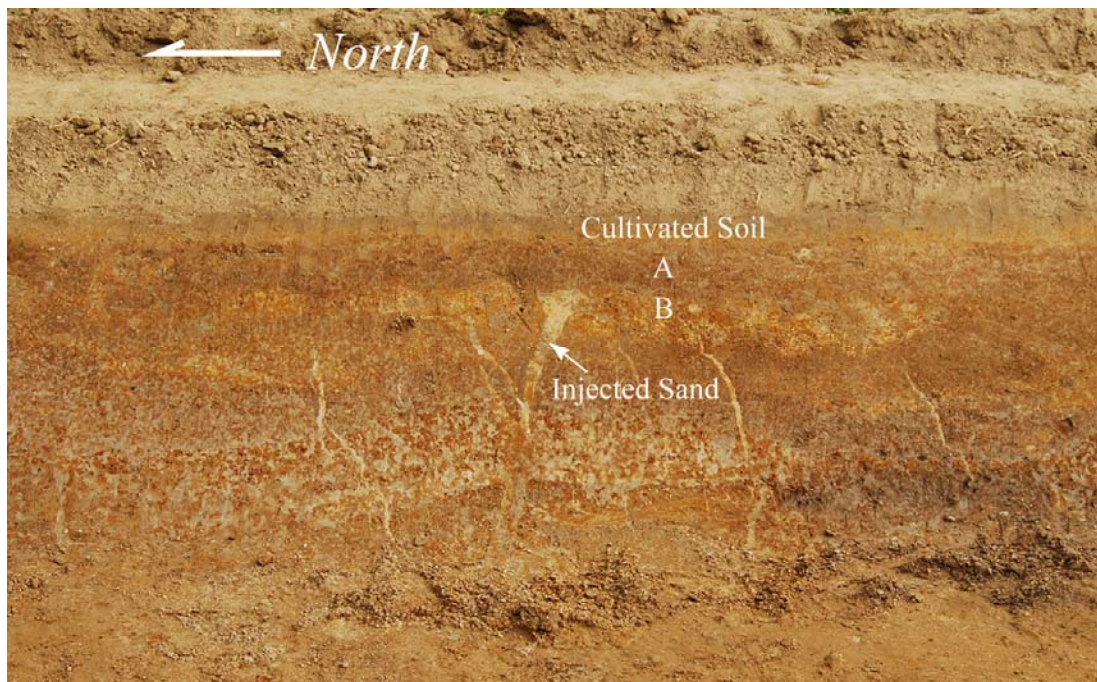
Figure 4-7 Sand Dikes induced by Liquefaction on the East Wall of the Trench

41
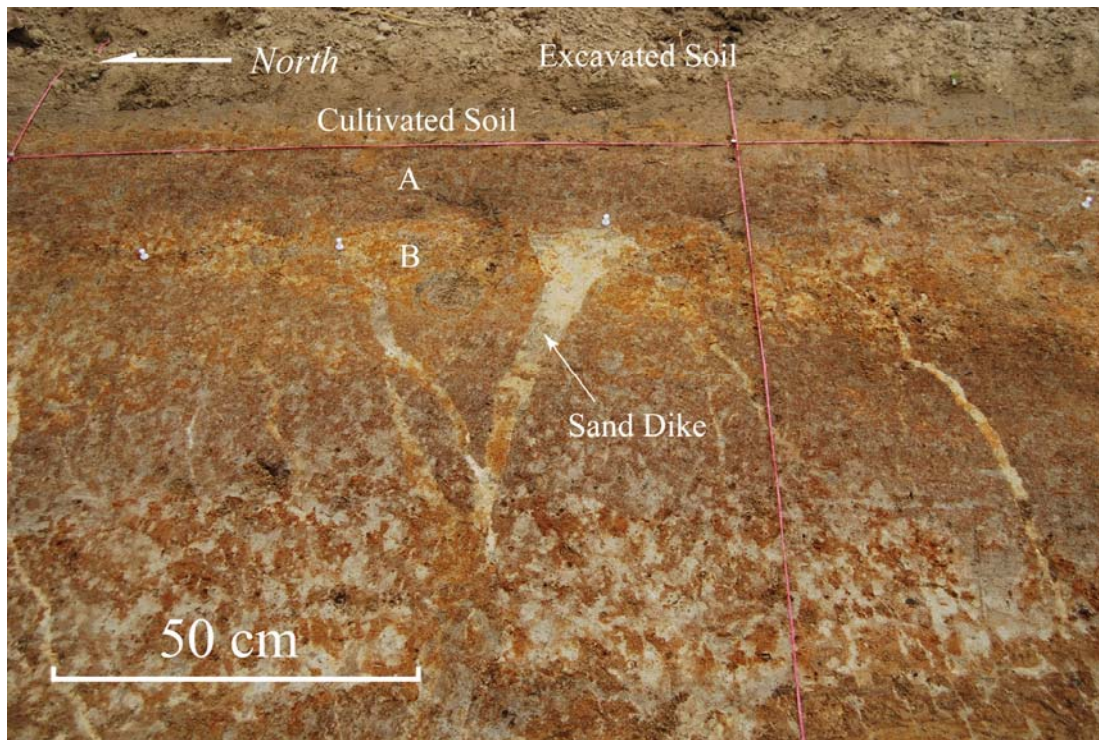
Figure 4-8   Close-View of Sand Dikes

Table 4-1   Result of ^{14}C Dating of Gabrakhari 1 Trench

Trench	Unit	Sample number	Laboratory number	Method	Material	Measured radiocarbon age (yBP)	δ 13C (permil)	Conventional radiocarbon age (yBP)	Calibrated Calender years (1 sigma)
Gabrakhari 1	A	Gab-1	Beta-253872	AMS	organic sediment	960 +/-40	-16.8	1090 +/- 40	AD 900 to 1000
	A	Gab-2	Beta-253873	AMS	organic sediment	770 +/-40	-18.2	880 +/- 40	AD 1060 to 1210
	B	Gab-3	Beta-253874	AMS	charred material	-	-	250 +/- 40	AD 1640 to 1660
	B	Gab-4	Beta-253875	AMS	charred material	-	-	2290 +/- 40	BC 400 to 370
	C	Gab-6	Beta-254557	AMS	charred material	80 +/- 40	-25.8	70 +/- 40	AD 1700 to 1960
	D	Gab-7	Beta-254558	AMS	organic sediment	70 +/- 40	-26.1	50 +/- 40	AD 1890 to 1960
	E	Gab-9	Beta-253877	AMS	charred material	120 +/- 40	-25.1	120 +/- 40	AD 1680 to 1960
	E	Gab-10	Beta-253878	AMS	charred material	200 +/- 40	-27.4	160 +/- 40	AD 1670 to 1950
	F	Gab-12	Beta-253880	AMS	charred material	100 +/- 0.5	-11.1	200 +/- 40	AD 1660 to 1950
	F	Gab-11	Beta-253879	AMS	charred material	290 +/- 40	-24.0	310 +/- 40	AD 1500 to 1650
	G	Gab-31	Beta-259993	AMS	peat	210 +/- 40	-26.3	190 +/- 40	AD 1660 to 1950
	G	Gab-32	Beta-258309	AMS	wood	410 +/- 40	-28.3	360 +/- 40	AD 1460 to 1630
	G	Gab-14	Beta-253882	AMS	peat	300 +/- 40	-23.0	330 +/- 40	AD 1480 to 1640
	I	Gab-15	Beta-253883	AMS	charred material	280 +/- 40	-26.1	260 +/- 40	AD 1640 to 1660

4.1.2. Trench Investigation at Gabrakhari 2 Site

The Gabrakhari 2 trench is located in the 300 m east of Gabrakhari 1 site. Though the Dauki Fault was confirmed at Gabrakhari 1 site, it was desired to confirm the fault at another site because of the importance. However, only gentle warping structure was recognized in the trench.

(1)   Stratigraphy identified in the Gabrakhari 2 Trench

The sedimentary succession in the trench is divided into units A to F. Unit E is divided into subunits E1 toE3 (Figure 4-9 and Figure 4-10).

Unit A: Blue clay

Unit B: Yellowish coarse sand

Unit C: Laminated sand

Unit D: Greenish silt

Unit E: This unit is divided into subunits E1, E2, and E3 on the west wall. Units E1 and E2 are composed of whitish clay. Unit E3 is composed of black peaty clay. The radiocarbon age of E3 on the east wall shows Cal AD 1650 to 1950 (see Table 4-2).

Unit F: Gray clay with fine to medium sand

(2)   Warping Structure

Units E2 and E3 on the west wall are gently warped (Figure 4-9 and Figure 4-11). Unit E3 on the east wall is also gently warped (Figure 4-10 and Figure 4-12). The warping structure is inferred to be formed by the activity of the Dauki Fault, since units E2 and E3 are composed of clay and silt and must have been deposited horizontally, though the inclination is very gentle. Units A to D cover unit E with unconformity.

(3)   Time of Seismic Event

The latest event, which formed the warping structure, is inferred to have occurred after the deposition of units E2 and E3. Since the radiocarbon age of unit E3 is Cal AD 1650 to 1950, the time of the latest event is after AD 1650. The candidate of the historical earthquakes along the Dauki Fault is only the 1548 earthquake and the 1664 earthquake except the 1897 earthquake. Therefore, this event may correspond with the 1897 earthquake.
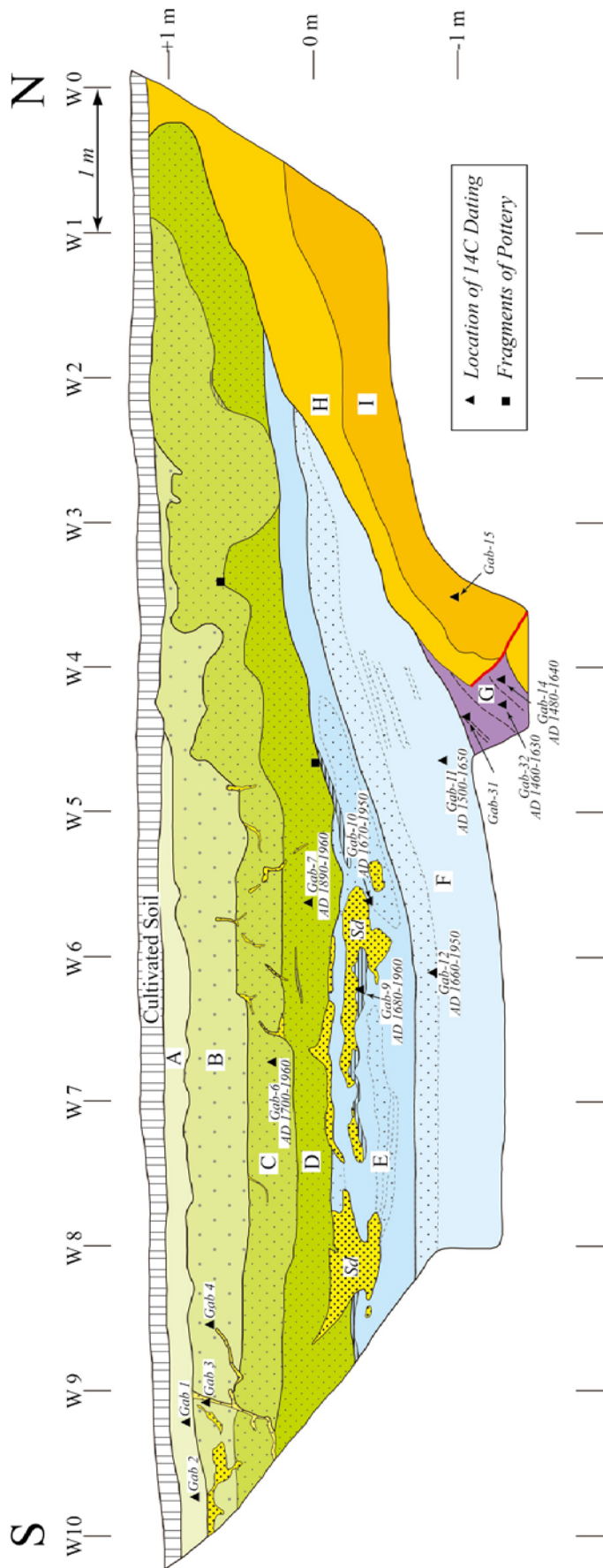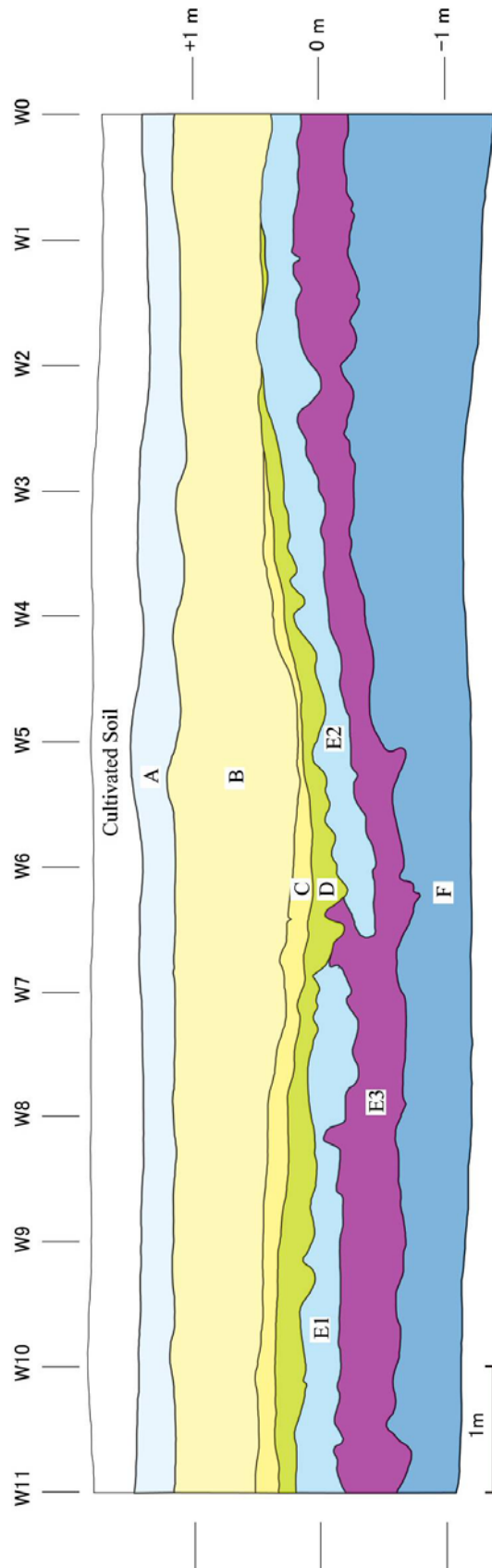
Figure 4-9   Log of the West Wall of Gabrakhari 2 Trench
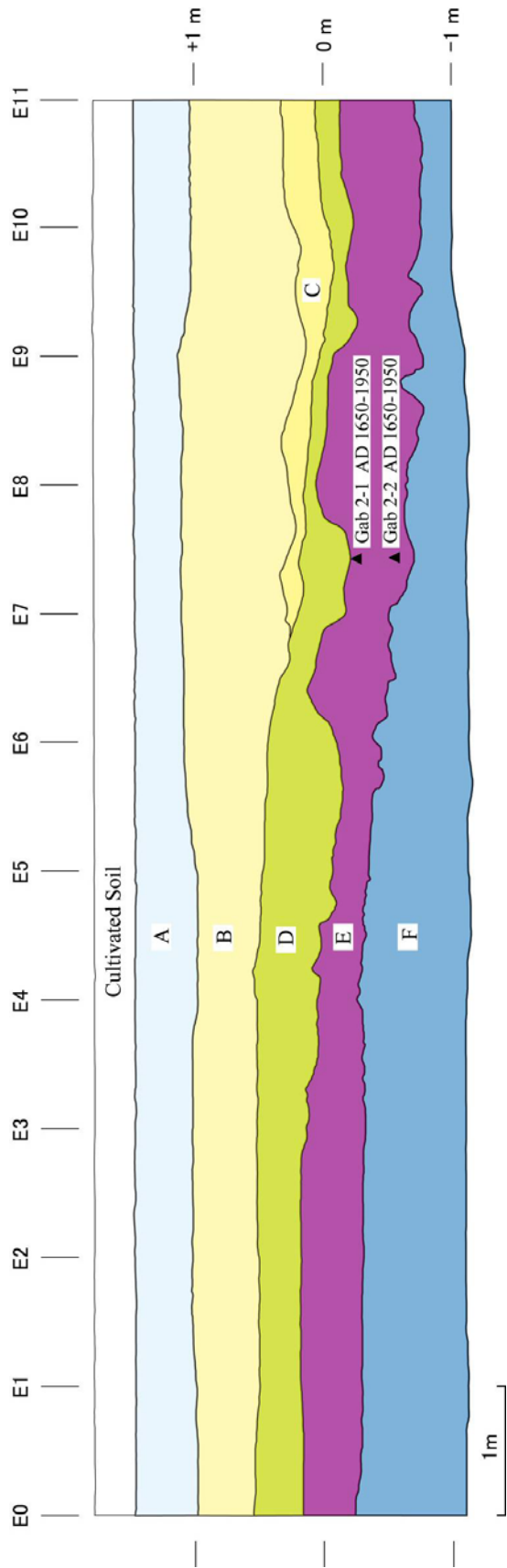
Figure 4-10   Log of the East Wall of Gabrakhari 2 Trench
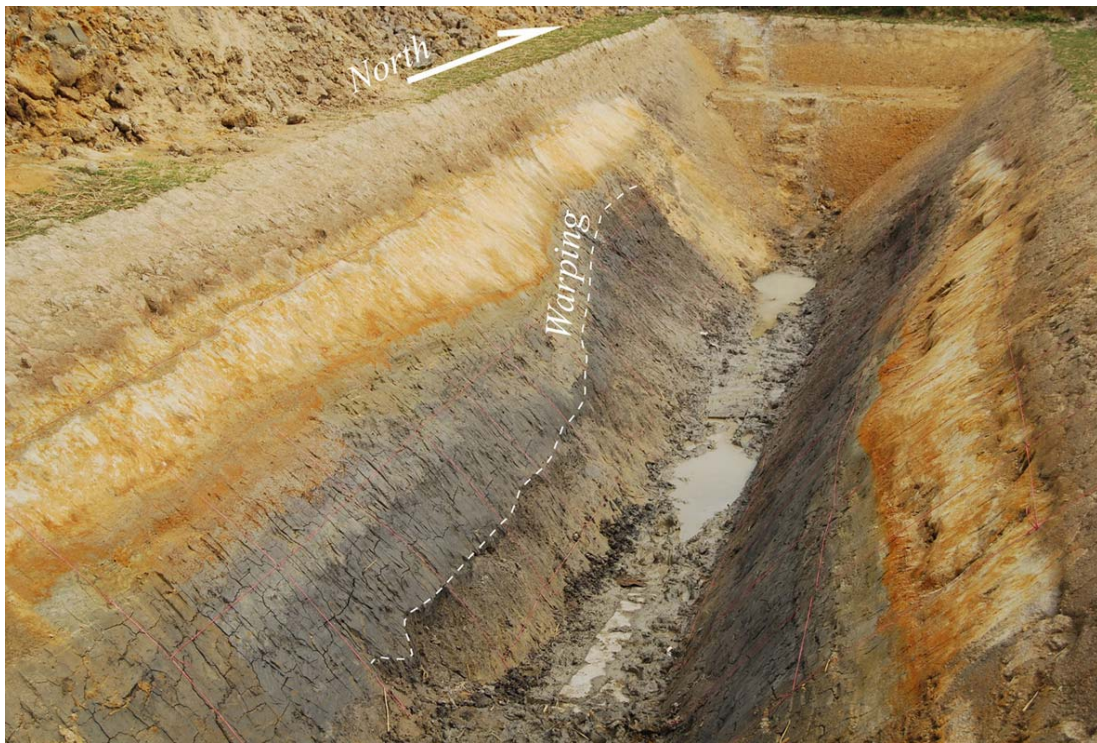
Figure 4-11   Photo of the West Wall at Gabrakhari 2 Trench
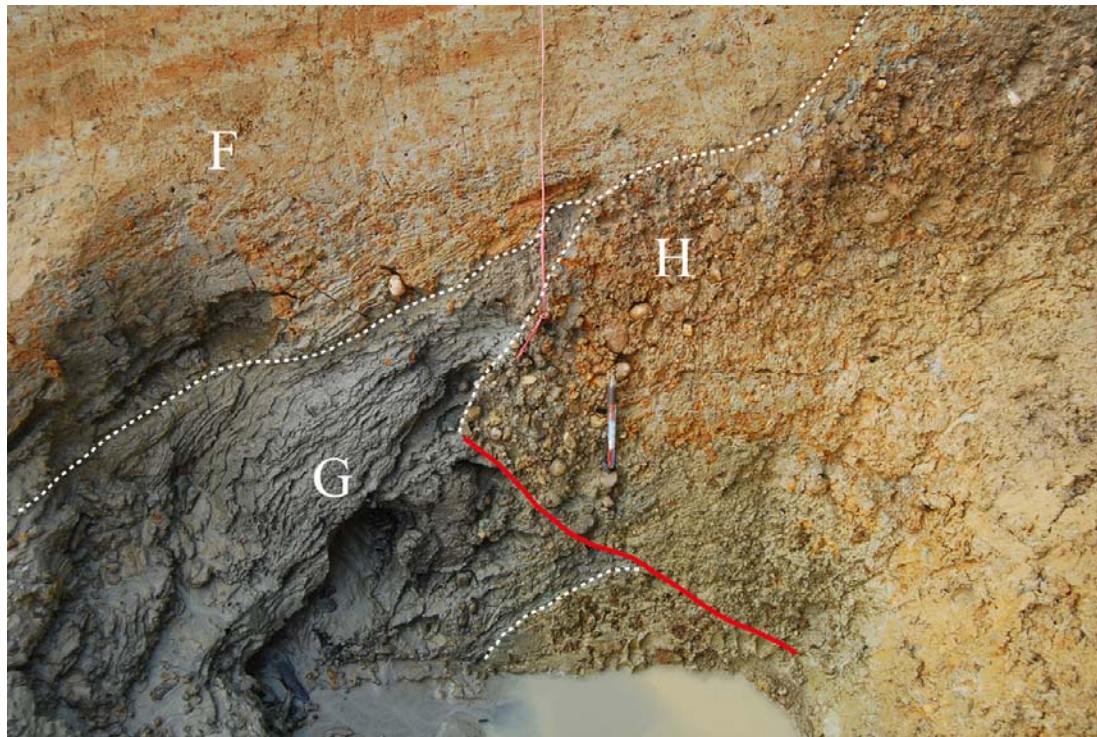

Figure 4-12   Photo of the East Wall at Gabrakhari 2 Trench

Table 4-2   Result of ^{14}C Dating of Gabrakhari 2 Trench

Trench	Unit	Sample number	Laboratory number	Method	Material	Measured radiocarbon age (yBP)	δ 13C (permil)	Conventional radiocarbon age (yBP)	Calibrated Calender years (1 sigma)
Gabrakhari 2	–	Gab 2-1	Beta-258308	AMS	charred material	20 +/- 40	-12.5	230 +/- 40	AD 1650 to 1950
	–	Gab 2-2	Beta-258307	AMS	charred material	30 +/- 40	-13.0	230 +/- 40	AD 1650 to 1950

4.1.3. Paleo-Liquefaction at Awlatory Village

Awlatory Village is located at about 2 km southeast of Gabrakhari Village (Figure 4-1). The sand dikes due to paleo-liquefaction were found out on the bank of the pond which was excavated in the alluvial plain (Figure 4-13 and Figure 4-14).　The small pit was excavated near the pond to observe the details of the liquefaction (Figure 4-15 and Figure 4-16). Many sand dikes intrude the alluvium and reach near the ground surface.　The alluvium is deformed by liquefaction (Figure 4-13).　The large liquefaction must have been generated by a large earthquake around Awlatory Village.

The alluvium near the bottom of the bank shows the radiocarbon age of Cal AD 1640 to 1660 (Table 4-3).　The sand dikes reach near the ground surface (Figure 4-15).　The alluvium near the surface must be younger than that of the bottom of the pond.　Therefore, it is suggested that the liquefaction occurred during the 1897 earthquake.

Figure 4-13　Sand Dikes at Awlatory Village

Figure 4-14　Close-View of Sand Dikes
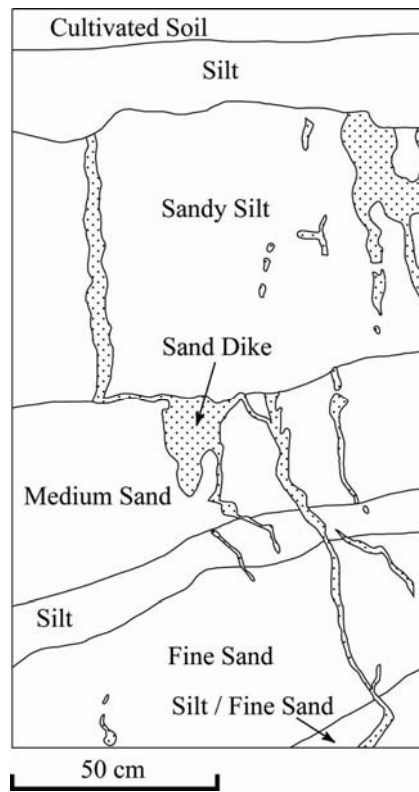
Figure 4-15   Sand Dikes in the Pit at Awlatory Village

Figure 4-16   Photo of the Sand Dikes in the Pit

Table 4-3   Result of ^{14}C Dating at Awlatory Village

Trench	Unit	Sample number	Laboratory number	Method	Material	Measured radiocarbon age (yBP)	δ 13C (permil)	Conventional radiocarbon age (yBP)	Calibrated Calender years (1 sigma)
Awlatory	–	AW–2	Beta–258305	AMS	charred material	NA	NA	260 +/– 40	AD 1640 to 1660
	–	AW–1	Beta–258306	AMS	charred material	NA	NA	420 +/– 40	AD 1440 to 1470

4.2. Trench Investigation across the Plate Boundary Fault at Feni

The trench was excavated at Loc.4-2 shown in Figure 3-9 and named Feni-1.   Another trench was excavated at Loc.4-3 shown in Figure 3-10 and named Feni-2.   The fault was concealed at both sites and only warping structure was observed.   In this report, the result of Feni-2 trench is mentioned.

(1)   Geomorphology around Feni-2 Trench Site

The topography around Feni-2 trench site is shown in Figure 4-17.   The flat surface on the right of the photo is uplifted terrace and the height is 1 to 3 m above the alluvial plain.   It is suggested that the topographic boundary between the uplifted terrace and the alluvial plain forms a low fault scarp or warping scarp.

(2)   Stratigraphy identified in the Trench

14 m long, 5 m wide, and 2 to 2.5 m deep trench was excavated with E-W direction. The log of the north wall is shown in Figure 4-18.   The photos of the north wall are shown in Figure 4-19 and Figure 4-20.   The result of ^{14}C dating is shown in Table 4-4.   The exposed sedimentary succession in the trench is divided into units A to E.

Unit A: Poorly stratified sandy clay
The stalks of plant were collected for the samples of ^{14}C dating, but the organic materials were found to be replaced by iron oxide, therefore, the dating was carried out with organic soil.   The dating of the organic soil showed older age, because the organic materials in the soil may have been reworked from the lower layers.

Unit B: Laminated sandy clay
The lamina is disturbed by the shaking of an earthquake.   This unit is gently inclined towards the west showing warping structure.   Though the ^{14}C dating was also carried out with the stalk of plant, the organic material was replaced by iron oxide.

Unit C: Alternation of clay and silt
This unit is gently inclined towards the west.   The samples of fragment of plant for ^{14}C dating were collected and the radiocarbon age shows 2020 ± 40 yBP (Cal BC 50 to AD 20) and 2040 ± 40 yBP (Cal BC 90 to AD 10).

Unit D: This unit is divided into subunits of Ds and Dg.   The layer is inclined towards the west with the inclination of 10° to 15° and is covered by unit

C with unconformity.　Ds consists of blue laminated silt.　The radiocarbon age of charcoal contained in the layer shows 1970 ± 40 yBP (Cal BC 10 to AD 70).　Dg consists of brown medium sand with gravel.

Unit E: Fine sand comprising the terrace

This unit is weakly consolidated by dehydration and oxidation near the ground surface on the east side of the trench, but the layer between N6 to N12 horizontal markers is not oxidized and soft at the bottom of the trench. T he sample, numbered Loc.2-21, shows younger age than that of unit D.　This sample may be the root of plant.

(3) Warping Structure and Event Horizon

The fault is concealed and only warping structure of the layers was observed in the trench.　Units B and C are gently inclined towards the west and the lamina of unit B is disturbed by the shaking of an earthquake.　Considering these observations, the latest event is inferred to have occurred after the deposition of unit B.

Unit C covers unit D with unconformity.　The penultimate event is inferred after the deposition of unit D and before the deposition of unit C.

(4) Time of Event

The time of the latest event is unknown, since the radiocarbon age of unit B is not obtained.　According to the age of units C and D, the time of the penultimate event is inferred to have occurred during Cal BC 90 and AD 70.
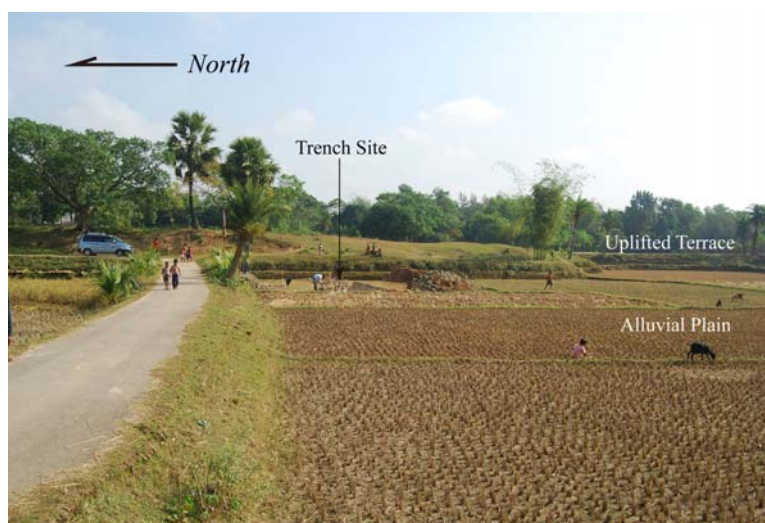
[The trench was excavated the topographic boundary between the uplifted terrace and alluvial plain.]

Figure 4-17　Photo of Feni-2 Trench Site
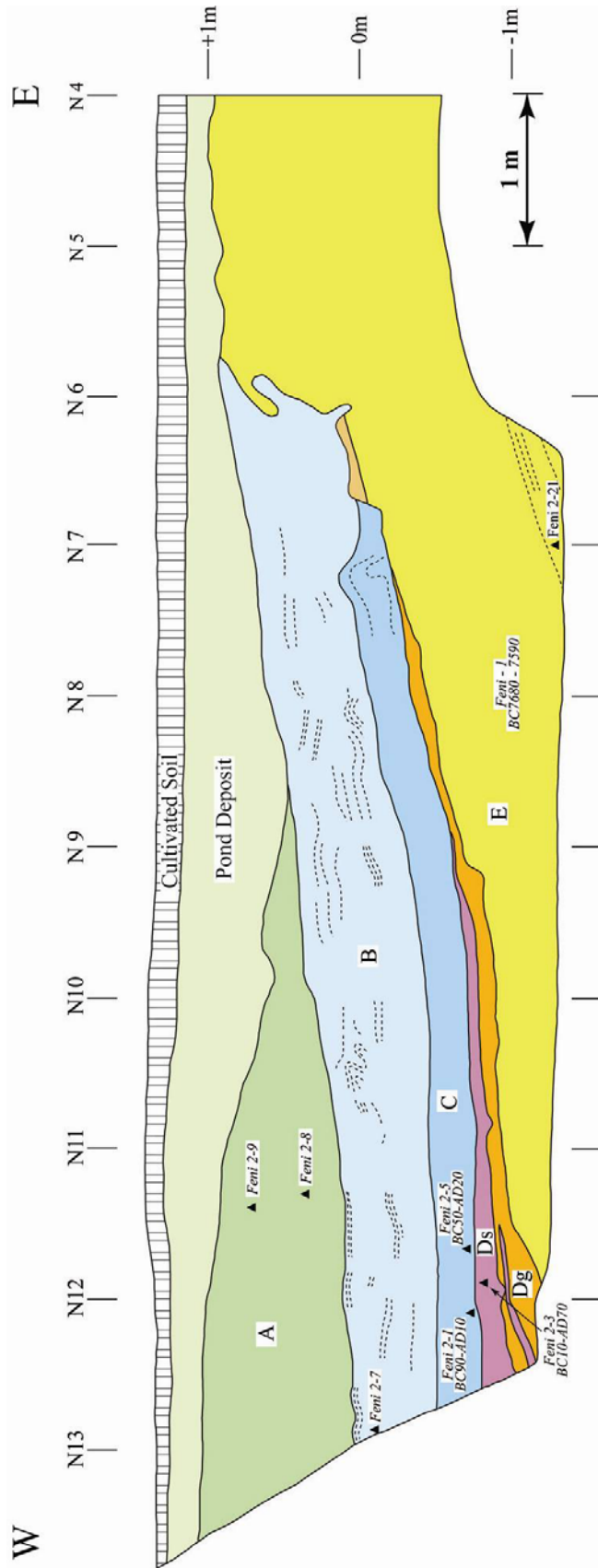
[Triangles represent the locations of ^{14}C dating.]

Figure 4-18   Log of the North Wall of Feni-2 Trench.

Figure 4-19   Photo of the North Wall of Feni-2 Trench taken from Southeast

Figure 4-20   Photo of the North Wall of Feni-2 Trench taken from Southwest

Table 4-4   Result of ^{14}C Dating of Feni-2 Trench

Trench	Unit	Sample number	Laboratory number	Method	Material	Measured radiocarbon age (yBP)	δ 13C (permil)	Conventional radiocarbon age (yBP)	Calibrated Calender years (1 sigma)
Feni 2	A	Feni 2-9	Beta–253869	AMS	organic sediment	8860 +/– 60	–21.6	8920 +/– 60	BC 8240 to 7970
		Feni 2-8	Beta–254559	AMS	organic sediment	7500 +/– 50	–20.9	7570 +/– 50	BC 6460 to 6410
	B	Feni 2-7	Beta–253868	AMS	organic sediment	10040 +/– 60	–18.3	10150 +/– 60	BC 10040 to 9760
	C	Feni 2-1	Beta–253864	AMS	plant material	2090 +/– 40	–28.2	2040 +/– 40	BC 90 to AD 10
		Feni 2-5	Beta–253866	AMS	plant material	2060 +/– 40	–27.4	2020 +/– 40	BC 50 to AD 20
	D	Feni 2-3	Beta–253865	AMS	charred material	2030 +/– 40	–28.4	1970 +/– 40	BC 10 to AD 70
	E	Feni 2-21	Beta–253870	AMS	plant material	910 +/– 40	–11.9	1120 +/– 40	AD 890 to 980
		Feni 1	Beta–253871	AMS	organic sediment	8560 +/– 50	–19.3	8650 +/– 40	BC 7680 to 7590

4.3. Crater confirmed at Hobigonj Village, Saestagonj

The very gentle warping scarp is identified on the alluvial plain 3-5 km west of the hill (see Figure 3-13). The trench investigation at two sites of A and B was carried out. However, an active fault could not be confirmed. It is thought that an active fault is concealed. Instead of the crater, which is a kind of liquefaction, was confirmed at Hobigonj Village. The crater was found out in the pit which was excavated by village person. The pit was excavated deeper with about 1m to detect the shape of the whole crater. The crater, which is a large liquefaction, must have been created near the epicenter of a large earthquake.

(1)   What is Crater?

According to McCalpin edited (1996), the crater is interpreted to have been formed in the following process:

1) A large hole is created at the surface by the violent upwards discharge of the liquefied mixture of sand and water.
2) A sand rim accumulates around the hole by continued expulsion of liquefied sand and water.
3) Sand, soil clasts, and water are churned briefly in the lower part of bowl, followed by settling of the large clasts and formation of the graded-fill sequence of sediment.
4) The crater is intermittently filled by the adjacent surface materials to form the thin stratified-filled sequence at the bottom and non-bedded organic matter rich sand during the weeks to years after the eruption.

(2)   Crater confirmed at Hobigonj Village

The photo of the crater is shown in Figure 4-21. S1 and S2, which show horizontal structure, are undisturbed layers. S1 layer is inferred to have been located near the ground surface during the formation of the crater, since S1 layer and the clast of S1 layer in the filled crater are weathered.

The bowl-shaped solid line represents the outline of the crater. The width of the top of the crater is about 3m. The whitish part ("liquefied sand" shown in Figure 4-21), which comprises of most of the crater, is the churned mixture of sand and water by continued expulsion after the eruption. Many clasts with size of 10 to 30 cm, which were fallen down from the wall of the crater, are contained in this layer. The crack like a normal fault is observed on the right wall of the crater (Figure 4-23). The clasts may have been fallen down into the crater along the crack like this. The sand dike intrudes into layer S1 on the left wall of the crater (Figure 4-22).

The dark part at the top of the crater is inferred to be the hole-filled deposits by the adjacent surface materials after the eruption (Figure 4-21).

(3)   Time of the Formation of the Crater

Two triangles of C and D shown in Figure 4-21 represent the location of the samples for ^{14}C dating.   The sample C is charcoal contained in the layer S1.   The sample D is charcoal contained in the hole-filled deposits after the eruption.   The radiocarbon age of the samples is shown in Table 4-4.   The radiocarbon ages of the sample C and D show Cal BC 1040 to 930 and Cal BC 1200 to 1040, respectively (Table 4-5).   The formation of the crater is dated back to about Cal BC 1000.   According to Shishikura et al. (2009), the fourth earthquake along the subduction fault is inferred to have occurred during Cal BC 1395 to 740 (refer to Table 5-1).   The crater may have been formed by this earthquake.

S1: weathered alternation of silt and fine sand
S2: fresh alternation of silt and fine sand
Solid white line shows the outline of the crater.
Broken white lines show clasts fallen down from the wall of crater.
   The clast in the center of the photo has inclined lamination, though the original structure of S1 and S2 is horizontal.   The dark part on the top of the crater is deposits which covered the hollow after the eruption.   Triangles represent the location of ^{14}C dating.]

Figure 4-21   Photo of the Crater confirmed at Hobigonj Village
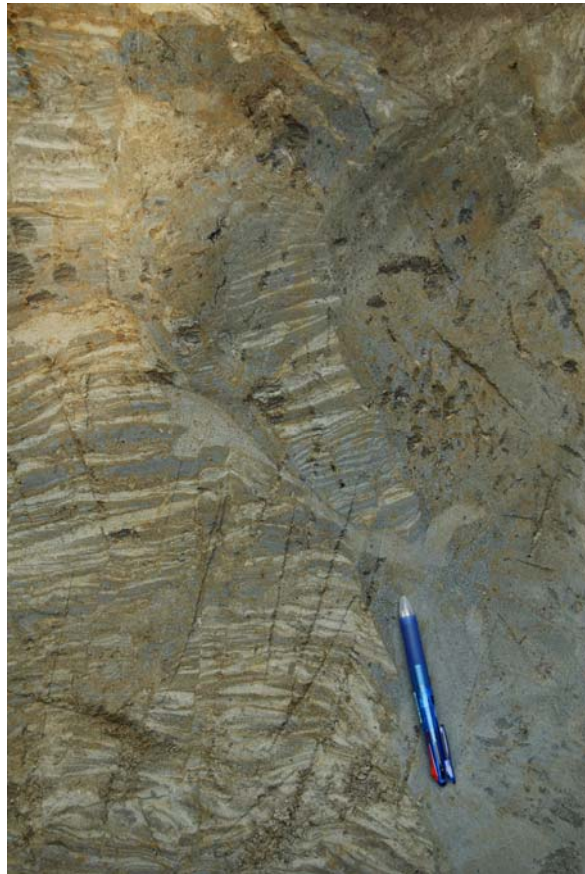
Figure 4-22   Close-View of the Left of the Crater

Figure 4-23   Close-View of the Right of the Crater

Table 4-5   Result of ^{14}C Dating at Hobigonj Village

Trench	Unit	Sample number	Laboratory number	Method	Material	Measured radiocarbon age (yBP)	δ 13C (permil)	Conventional radiocarbon age (yBP)	Calibrated Calender years (1 sigma)
Hobigonj	–	Hob-D	Beta-258303	AMS	plant	2970 +/–460	–27.9	2920 +/– 40	BC 1200 to 1040
	–	Hob-C	Beta-258304	AMS	plant	2910 +/– 40	–29.4	2840 +/– 40	BC 1040 to 930

4.4. Saidpur Site

The small trench (pilot trench) was excavated in Saidpur, since the rice before harvest was planted at the trench site. A little possibility of active fault, but the future detailed survey is expected for clarification during December to January when the rice is not planted.

5. Time-Predictable Model for Each Fault

Characteristic earthquake is defined as the one that has a certain recurrence period and displacement on the specific fault.   It is well-known that active fault generates characteristic earthquakes.   If the time of the latest and penultimate events on the active fault is revealed, the recurrence period and the elapsed time since the latest event are known and the probability of future earthquake occurrence can be estimated.   This is a kind of prospect of future earthquake occurrence based on the time- predictable model.   However, the earthquakes which occur in the interval of characteristic earthquakes, though the magnitude is less than that of characteristic earthquakes, are also known.   In this report, this is named as non-characteristic earthquake.

To suggest the time-predictable model on an active fault, the time of at least two paleo-earthquakes should be known.   However, in Bangladesh, the documents on the historical earthquake are limited only for around 150 years, that is not sufficient.   And the number of trench investigation is less.   Under the present condition, it is difficult to build certain time-predictable model for each active fault.   The time-predictable model for each active fault will be suggested on the basis of the present information and the model should be revised in the future.

Although above limited condition, the time of events, recurrence period, elapsed time since the latest event and the 50 years probability of future earthquake occurrence for each active fault are estimated using current limited information and are shown in Table 5-1.   The Brownian Passage Time model (BPT model) is adopted as the probability density function. The aperiodicity α is presumed to be 0.5 followed after Parsons (2004) etc.

Table 5-1   Time-Predictable Model and 50 Years Probability

Segment		Events	Observed Recurrence Period (years)	Elapsed Time since Last Event (years)	50 year Prob. Time-Dependent (%)	Estimated Magnitude (Mw)	Length (km)
Plate Boundary Fault (PBF)	PBF-1	**AD 1762**[1] AD 680 to 980[1] BC 150 to AD 60[1,2] BC 1395 to 740[1]	900	246	1.1	8.5	795
	PBF-2	before 16th century	> 900	> 508	> 6.7	8.0	270
	PBF-3	before 16th century	> 900	> 508	> 6.7	8.3	504
Dauki Fault (DF)		**AD 1897**[3] AD 1500 to 1630[3] (AD 1548 ?)	349	111	7.0	8.0	233
Madhupur Blind Fault (MF)		**AD 1885**	350	123	8.7	7.5[4]	60
Non-characteristic but relating to fault[5] (PBF-2, PBF-3, DF)		AD 1918 (PBF-2) AD1869, 1943, 1954, 1988 (PBF-3) AD 1664, 1923, 1930 (DF)	20	–	–	7.0 – 7.4	–

1) Shishikura et al. (2009)
2) Based on the trench investigation of this project at Feni
3) Based on the trench investigation of this project at northeast of Haluaghat
4) AD 1885 earthquake was M=6.9~7.0, but possibly M=7.5 in the future
5) M=7.0 to 7.4 earthquakes have often occurred in the interval of characteristic earthquakes, and may not repeat on a specific fault and occurs randamly

(1)   Subduction Fault and the Northern Extension

The subduction fault and the northern extension are temporarily divided into segments PBF1 to PBF3 (Figure 3-1).   PBF1 is subduction fault which extends off Myanmar to off Chittagong and Feni.   PBF2 is the inland northern extension of subduction fault which extends Comilla to Sylhet.   PBF3 is the plate boundary fault inferred from Sylhet to Assam, India.

PBF1

Shishikura et al. (2008, 2009) suggested four times paleo-earthquakes on the PBF1, viz. AD 1585 to 1810, AD 680 to 980, BC 150 to AD 60, and BC 1395 to 740 based on the studies of uplifted marine terraces at off Myanmar islands.   The latest event during AD 1585 to 1810 corresponds with the 1762 earthquake.   The recurrence period estimated from these four times events is about 900 years.   The event during BC 90 to AD 70 at Feni-2 trench site corresponds with the third event by Shishikura et al. (2009).   The 50 years probability of future earthquake occurrence is 1.1 %, which is small, because the elapsed time since the latest event is 246 years and the recurrence period is 900 years.

PBF2

It can be suggested that the 1548 earthquake may be the latest event on the PBF2, since Sylhet and Chittagong suffered severe damage with this earthquake. However, it is suspicious, the historical documents related to the earthquake and damage are insufficient.   According to the trench investigation at Gabrakhari Village across the Dauki Fault, it is inferred that the 1548 event was generated by the activity of the Dauki Fault.   Therefore, the latest event and the recurrence period along the PBF2 are unknown.   More trench investigation across the PBF2 is necessary.   If the recurrence period is 900 years by analogy with PBF1 and the latest event is before 16th century, 50 years probability is over 6.7 %.

The 1918 earthquake (Ms 7.6) occurred around PBF2, however. the magnitude is small comparing to the empirically estimated magnitude (Mw 8.0) from fault length (Wells and Coppersmith, 1994) and the damage was not severe.   Therefore, the 1918 earthquake is not treated as a characteristic earthquake.

PBF3

Several historical earthquakes occurred around the PBF3, viz. the 1869 earthquake (Ms 7.5), the 1943 earthquake, the 1954 earthquake (Ms 7.4), and the 1988 earthquake (Ms 6.6).   However, these earthquakes are not treated as characteristic earthquakes, since the magnitude is small comparing to the empirically estimated magnitude (Mw8.3) from the fault length.   The time of the latest event and the

recurrence period are unknown.   If the latest event is before 16th century and the recurrence period is 900 years, 50 year probability is over 6.7 %.

(2)   Dauki Fault (DF)

The time of two paleo-earthquakes was identified by the trench investigation at Gabrakhari Village and paleo-liquefaction at Awlatory Village.   The time of the latest event is AD 1700 to 1960.   The latest event corresponds with the 1897 Great Assam Earthquake.   The time of the penultimate event is AD 1500 to 1630.   It is inferred that this event corresponds with the 1548 earthquake.   Since the recurrence period is 349 years and the elapsed time is 111 years, the 50 years probability is 7.0 %.   The recurrence period of the Dauki Fault is similar to that of the active faults of Himalaya.

(3)   Madhupur Blind Fault (MF)

The 1885 earthquake (Ms 7.0) is regarded as the latest event for characteristic earthquake on the Madhupur Fault based on the existing documents.   The recurrence period is unknown.   If the recurrence period is 350 years by analogy with the Dauki Fault, the 50 years probability is 8.7 %.   The Madhupur Fault is suggested to be a blind fault, therefore, the trench investigation is not effective. The seismic reflection survey and drilling are necessary to detect the faulting history along the Madhupur Fault.

(4)   Non-Characteristic Earthquake

The earthquakes with smaller magnitude comparing to characteristic earthquakes frequently occurred in historical period.   These earthquakes can not be neglected for seismic hazard assessment.

6. Recommendation for Future Survey

For the analysis of time-predictable model, the time of at least two events, the latest event and the penultimate event, must be identified, and then the recurrence period and the elapsed time since the latest event should be clarified. Further for a long active fault, the segmentation model based on the faulting history should be discussed. If the long-period historical documents are available such as the North Anatolian Fault in Turkey, the time-predictable model can be analyzed by the historical earthquakes. However, the historical documents in Bangladesh are not sufficient for the analysis of the time-predictable model. Therefore, it is indispensable to carry out the trench investigation at many sites.

The trench investigations mentioned in this report were first ones carried out in Bangladesh. The study of active fault based on trench investigation should be progressed in future.

1) On the subduction fault from off Myanmar to off Chittagong, the faulting history is estimated by the study of the uplifted marine terraces (Shishikura et al., 2008, 2009). However, on the inland northern extension of the subduction fault, the nature of the fault and the faulting history are not clarified, for example the northern limit of the subduction fault and the segmentation model of the plate boundary fault. On the plate boundary from Saestagonj to Sylhet, even the location of active fault is not understood. The quality of the CORONA images in this area is not good due to many clouds. The satellite photo interpretation should be re-examined using other satellite images (e.g. ALOS or SPOT image) and more trench investigation across the plate boundary fault is necessary.

2) According to the trench investigation at Gabrakhari, it is revealed that the Dauki Fault has ruptured during the 1897 earthquake, and the recurrence period, which is about 350 years, is similar to that of active fault in Himalaya. The faulting history should be confirmed at another region, e.g. north of Sherpur.

3) The most part of the subduction fault is distributed in the ocean. Therefore, the study of the uplifted marine terrace is quite important to clarify the faulting history of the subduction fault. Dr. Shishikura and Dr. Morino visited Teknaf, southeast Bangladesh, on January 2009 for reconnaissance and identified uplifted marine terraces. The detailed survey on the uplifted marine terrace is necessary.

4) The fault topography in Bangladesh is severely modified by the cultivation and the construction of road. Since the trench is excavated across a low scarp, the modification makes the trench investigation a difficult task. If the location of active

fault is inferred by shallow seismic reflection survey, the trench investigation may become easily.   The application of shallow seismic reflection survey should be considered.

5) It is supposed that Madhupur Fault is a blind fault, consequently, it is difficult to adopt trench investigation.   Hence, the seismic reflection survey and drilling are necessary to detect the Madhupur Fault.

6) Regarding to blind active fault ,mapping, other and further investigation should be conducted such as seismic reflection and drilling survey.

[References]

Alam, A. K. M. K, 2001, Geomorphology and neotectonics along some faults in Bangladesh. Bangladesh Geoscience Journal, 7, 51-62.

Ambraseys N. N. (2004). Three little known early earthquakes in India. current science, 86, 506-508.

Bilham, R., and P. England, (2001). Plateau pop-up during the great 1897 Assam earthquake. Nature, 410, 806-809.

Bilham, R. (2004). Earthquakes in India and the Himalaya tectonics, geodesy and history. Annals of Geophysics, 47, 839-858.

Bilham, R., and S. Hough. (2006). Future Earthquakes on the Indian Subcontinent: Inevitable Hazard, Preventable Risk. South Asian Journal, 12, 1-9.

McCalpin, J. P. edited (1996). Paleoseismology; Academic Press New York p.588.

Nakata, T. and Y. Kumahara, 2002, Active faulting across the Himalaya and its significance in the collision tectonics. Active Fault Research, 20, 7-16.

Oldham, T. (1883). A catalogue of Indian earthquakes. Mem. Geol. Surv. India, 19, 163-215, Geol. Surv. India, Calcutta.

Persons, T. (2004). Recalculated probability of M$\geq$7 earthquakes beneath the Sea of Marmara, Turkey. J. Geophys. Res., 109, B05304, doi:10.1029/2003JB002667.

Sabri, M.S.A. (2001). Earthquake intensity-attenuation relationship for Bangladesh and its surrounding region. master thesis, Bangladesh University of Engineering and Technology, Dhaka, Bangladesh.

Shishikura, M., Y. Okamura, S. Fujino, W. Naing, S. T. Tun., and T. Aung. (2008). Two types of paleo-earthquakes recorded on marine terrace and fossil in the Mumaung Island, western Myanmar. AOGS 5th Annual Meeting (Busan), SE84-A015.

Shishikura, M., Y. Okamura, K. Satake, S. Fujino, T. T. Aung, W. Swe, W. Naing, H. Soe, S. T. Tun, T. L. Swe., and T. Aung. (2009). Geomorphological evidence of great Holocene earthquakes off western Myanmar. Proceedings of the international workshop on Tsunami and storm surge hazard assessment and management for Bangladesh, 22

Utsu, T. (2002). A list of deadly earthquakes in the World: 1500-2000, in Lee, W.K., Kanamori, H., Jennings, P.C., and Kisslinger, C., eds., International handbook of earthquake engineering and seismology: Amsterdam, Academic Press, p. 691-717.

Wells, D. L. and K. J. Coppersmith. (1994). New Empirical Relationships among Magnitude, Rupture Length, Rupture Width, Rupture Area, and Surface Displacement. Bull. Seismol. Soc. Am., 84, 974-1002.

Yeats, R. S., K. Sieh, and C. R. Allen. (1997). The geology of earthquakes. Oxford University Press, 568p.

Appendix: Information of CORONA Satellite Image

Satellite Image	CORONA
Organization	U.S. Geological Survey
Products Description	Product Descrition: High Resolution Scanned 70MM X 29.8 in. B/W

No.	Entity ID	Acquisition Date
1	DS1106-2055DF201	1969/02/09
2	DS1106-2055DF203	1969/02/09
3	DS1106-2055DF204	1969/02/09
4	DS1106-2055DF205	1969/02/09
5	DS1106-2055DF206	1969/02/09
6	DS1106-2055DF207	1969/02/09
7	DS1045-2117DA022	1968/02/01
8	DS1045-2117DA023	1968/02/01
9	DS1045-2117DA026	1968/02/01
10	DS1045-2117DA027	1968/02/01
11	DS1045-2117DA029	1968/02/01
12	DS1045-2117DA030	1968/02/01
13	DS1045-2117DA031	1968/02/01
14	DS1045-2117DA021	1968/02/01
15	DS1045-2117DA025	1968/02/01
16	DS1045-2117DA028	1968/02/01
17	DS1045-2117DA024	1968/02/01
18	DS1045-2117DF022	1968/02/01
19	DS1045-2117DF027	1968/02/01
20	DS1045-2117DF032	1968/02/01
21	DS1045-2117DF021	1968/02/01
22	DS1045-2117DF023	1968/02/01
23	DS1045-2117DF024	1968/02/01
24	DS1045-2117DF025	1968/02/01
25	DS1045-2117DF026	1968/02/01
26	DS1045-2117DF028	1968/02/01
27	DS1045-2117DF029	1968/02/01
28	DS1045-2117DF030	1968/02/01
29	DS1045-2117DF031	1968/02/01
30	DS1106-2055DF202	1969/02/09
31	DS1106-2055DF200	1969/02/09

No.	Entity ID	Acquisition Date
32	DS1106-2055DA206	1969/02/09
33	DS1106-2055DA207	1969/02/09
34	DS1106-2055DA209	1969/02/09
35	DS1106-2055DA211	1969/02/09
36	DS1106-2055DA212	1969/02/09
37	DS1106-2055DA210	1969/02/09
38	DS1106-2055DA208	1969/02/09
39	DS1106-2055DA213	1969/02/09
40	DS1116-1039DA040	1972/04/22
41	DS1116-1039DA041	1972/04/22
42	DS1116-1039DA042	1972/04/22
43	DS1116-1039DA043	1972/04/22
44	DS1116-1039DA045	1972/04/22
45	DS1116-1039DA046	1972/04/22
46	DS1116-1039DA049	1972/04/22
47	DS1116-1039DA050	1972/04/22
48	DS1116-1039DA054	1972/04/22
49	DS1116-1039DA055	1972/04/22
50	DS1116-1039DA056	1972/04/22
51	DS1116-1039DA059	1972/04/22
52	DS1116-1039DA060	1972/04/22
53	DS1116-1039DA063	1972/04/22
54	DS1116-1039DA064	1972/04/22
55	DS1116-1039DA066	1972/04/22
56	DS1116-1039DA067	1972/04/22
57	DS1116-1039DA068	1972/04/22
58	DS1116-1039DA070	1972/04/22
59	DS1116-1039DA072	1972/04/22
60	DS1116-1039DA053	1972/04/22
61	DS1116-1039DA044	1972/04/22
62	DS1116-1039DA047	1972/04/22
63	DS1116-1039DA051	1972/04/22
64	DS1116-1039DA057	1972/04/22
65	DS1116-1039DA061	1972/04/22
66	DS1116-1039DA065	1972/04/22
67	DS1116-1039DA069	1972/04/22
68	DS1116-1039DA073	1972/04/22

No.	Entity ID	Acquisition Date
69	DS1116-1039DA058	1972/04/22
70	DS1116-1039DA039	1972/04/22
71	DS1116-1039DA048	1972/04/22
72	DS1116-1039DA062	1972/04/22
73	DS1116-1039DA071	1972/04/22
74	DS1116-1039DA052	1972/04/22
75	DS1116-1039DF034	1972/04/22
76	DS1116-1039DF036	1972/04/22
77	DS1116-1039DF037	1972/04/22
78	DS1116-1039DF041	1972/04/22
79	DS1116-1039DF042	1972/04/22
80	DS1116-1039DF043	1972/04/22
81	DS1116-1039DF044	1972/04/22
82	DS1116-1039DF047	1972/04/22
83	DS1116-1039DF049	1972/04/22
84	DS1116-1039DF050	1972/04/22
85	DS1116-1039DF051	1972/04/22
86	DS1116-1039DF052	1972/04/22
87	DS1116-1039DF053	1972/04/22
88	DS1116-1039DF054	1972/04/22
89	DS1116-1039DF056	1972/04/22
90	DS1116-1039DF057	1972/04/22
91	DS1116-1039DF058	1972/04/22
92	DS1116-1039DF059	1972/04/22
93	DS1116-1039DF060	1972/04/22
94	DS1116-1039DF061	1972/04/22
95	DS1116-1039DF063	1972/04/22
96	DS1116-1039DF065	1972/04/22
97	DS1116-1039DF066	1972/04/22
98	DS1116-1039DF067	1972/04/22
99	DS1116-1039DF062	1972/04/22
100	DS1116-1039DF045	1972/04/22
101	DS1116-1039DF033	1972/04/22
102	DS1116-1039DF039	1972/04/22
103	DS1116-1039DF035	1972/04/22
104	DS1116-1039DF040	1972/04/22
105	DS1116-1039DF038	1972/04/22

No.	Entity ID	Acquisition Date
106	DS1116-1039DF048	1972/04/22
107	DS1116-1039DF055	1972/04/22
108	DS1116-1039DF064	1972/04/22
109	DS1116-1039DF046	1972/04/22
110	DS1017-2086DF174	1965/03/03
111	DS1017-2086DF177	1965/03/03
112	DS1017-2086DF178	1965/03/03
113	DS1017-2086DF179	1965/03/03
114	DS1017-2086DF180	1965/03/03
115	DS1017-2086DF181	1965/03/03
116	DS1017-2086DF183	1965/03/03
117	DS1017-2086DF184	1965/03/03
118	DS1017-2086DF187	1965/03/03
119	DS1017-2086DF188	1965/03/03
120	DS1017-2086DF189	1965/03/03
121	DS1017-2086DF190	1965/03/03
122	DS1017-2086DF191	1965/03/03
123	DS1017-2086DF192	1965/03/03
124	DS1017-2086DF194	1965/03/03
125	DS1017-2086DF195	1965/03/03
126	DS1017-2086DF197	1965/03/03
127	DS1017-2086DF198	1965/03/03
128	DS1017-2086DF199	1965/03/03
129	DS1017-2086DF200	1965/03/03
130	DS1017-2086DF186	1965/03/03
131	DS1017-2086DF196	1965/03/03
132	DS1017-2086DF182	1965/03/03
133	DS1017-2086DF175	1965/03/03
134	DS1017-2086DF176	1965/03/03
135	DS1017-2086DF185	1965/03/03
136	DS1017-2086DF193	1965/03/03
137	DS1017-2086DF201	1965/03/03
138	DS1017-2086DA181	1965/03/03
139	DS1017-2086DA182	1965/03/03
140	DS1017-2086DA183	1965/03/03
141	DS1017-2086DA184	1965/03/03
142	DS1017-2086DA185	1965/03/03

No.	Entity ID	Acquisition Date
143	DS1017-2086DA186	1965/03/03
144	DS1017-2086DA187	1965/03/03
145	DS1017-2086DA190	1965/03/03
146	DS1017-2086DA192	1965/03/03
147	DS1017-2086DA194	1965/03/03
148	DS1017-2086DA195	1965/03/03
149	DS1017-2086DA196	1965/03/03
150	DS1017-2086DA200	1965/03/03
151	DS1017-2086DA202	1965/03/03
152	DS1017-2086DA204	1965/03/03
153	DS1017-2086DA205	1965/03/03
154	DS1017-2086DA198	1965/03/03
155	DS1017-2086DA179	1965/03/03
156	DS1017-2086DA178	1965/03/03
157	DS1017-2086DA191	1965/03/03
158	DS1017-2086DA188	1965/03/03
159	DS1017-2086DA199	1965/03/03
160	DS1017-2086DA203	1965/03/03
161	DS1017-2086DA180	1965/03/03
162	DS1017-2086DA189	1965/03/03
163	DS1017-2086DA201	1965/03/03
164	DS1017-2086DA197	1965/03/03
165	DS1017-2086DA193	1965/03/03
166	DS1029-1038DF087	1966/02/05
167	DS1029-1038DF088	1966/02/05
168	DS1029-1038DF090	1966/02/05
169	DS1029-1038DF091	1966/02/05
170	DS1029-1038DF086	1966/02/05
171	DS1029-1038DF089	1966/02/05
172	DS1029-1038DF092	1966/02/05
173	DS1029-1038DA090	1966/02/05
174	DS1029-1038DA091	1966/02/05
175	DS1029-1038DA092	1966/02/05
176	DS1029-1038DA093	1966/02/05
177	DS1029-1038DA094	1966/02/05
178	DS1029-1038DA095	1966/02/05
179	DS1029-1038DA089	1966/02/05

No.	Entity ID	Acquisition Date
180	DS1025-2134DA097	1965/10/14
181	DS1025-2134DA098	1965/10/14
182	DS1025-2134DA101	1965/10/14
183	DS1025-2134DA102	1965/10/14
184	DS1025-2134DA103	1965/10/14
185	DS1025-2134DA104	1965/10/14
186	DS1025-2134DA105	1965/10/14
187	DS1025-2134DA106	1965/10/14
188	DS1025-2134DA100	1965/10/14
189	DS1025-2134DA099	1965/10/14
190	DS1025-2134DF091	1965/10/14
191	DS1025-2134DF093	1965/10/14
192	DS1025-2134DF094	1965/10/14
193	DS1025-2134DF096	1965/10/14
194	DS1025-2134DF098	1965/10/14
195	DS1025-2134DF095	1965/10/14
196	DS1025-2134DF099	1965/10/14
197	DS1025-2134DF097	1965/10/14
198	DS1025-2134DF100	1965/10/14
199	DS1025-2134DF092	1965/10/14